Global and Planetary Change 212 (2022) 103797

Contents lists available at ScienceDirect

Global and Planetary Change

journal homepage: www.elsevier.com/locate/gloplacha

Streamflow frequency changes across western Europe and interactions with North Atlantic atmospheric circulation patterns

J. Lorenzo-Lacruz [a,*], E. Morán-Tejeda [b], S.M. Vicente-Serrano [c], J. Hannaford [d], C. García [b], D. Peña-Angulo [c], C. Murphy [e]

[a] Department of Human Sciences, Area of Physical Geography, University of La Rioja, Logroño, Spain
[b] Department of Geography, University of the Balearic Islands, Palma, Spain
[c] Pyrenean Institute of Ecology, Spanish Research Council, Zaragoza, Spain
[d] Centre for Ecology and Hydrology, Wallingford, United Kingdom
[e] Irish Climate Analysis and Research Unit (ICARUS), Department of Geography, Maynooth University, Maynooth, Ireland

ARTICLE INFO

Editor: Dr. Howard Falcon-Lang

Keywords:
Wavelets
Climate modes
Streamflow
Periodicities
Synchronicities
Non-stationarity

ABSTRACT

This study identifies significant periodicities in streamflow dynamics across western Europe using a hydrological database encompassing 1874 monthly series from catchments in Ireland, the United Kingdom, France, Spain and Portugal, spanning the years 1962 to 2012. Significant and synchronous periodicities with the main atmospheric mechanisms over the North Atlantic sector are also identified using Cross Wavelet Transform and Wavelet Coherence analysis. Principal Components Analysis (PCA) were applied to the different Wavelet transforms analysis in order to summarize the results. These show the occurrence of a 7-years streamflow cycle in a large proportion of catchments within the study domain since the mid 1980's that was not present in earlier periods. The significance, intensity and persistence of the observed regional cycle follows a spatial gradient around the English Channel. We show how the transitive coupling of key atmospheric mechanisms is an influencing factor causing the general change observed. These results suggest the occurrence of a regional change in the periodicities of streamflow across the western European domain. Our results emphasize the non-stationary interaction between streamflow and atmospheric circulation during recent decades and the prominent role of the North Atlantic Oscillation in the newly stablished streamflow cycles.

1. Introduction

Recent climate changes are altering terrestrial hydrological systems worldwide (Haunschild et al., 2016). In Europe, significant changes in streamflow have been observed in recent decades (García-Ruiz et al., 2011; Masseroni et al., 2020; Van Loon et al., 2012; Vicente-Serrano et al., 2011a), with the role of climate variability, anthropogenic water uses and land cover changes having contrasting impacts in North and South West Europe (Teuling et al., 2019; Vicente-Serrano et al., 2019). The most notable changes observed in European streamflow are characterized by the diverging regional trends in historical records, with increasing trends in the north as a consequence of increased precipitation and a generalized decrease in the south of the continent as consequence of land cover changes and enhanced water uses (Hannaford, 2015; Kahya and Kalayci, 2004; Lorenzo-Lacruz et al., 2012; Masseroni et al., 2020; Morán-Tejeda et al., 2012; Stahl et al., 2010).

Different studies have stressed the important role of atmospheric circulation mechanisms in explaining temporal variability and recent trends identified in Western Europe (Bierkens and Van Beek, 2009; Hannaford and Buys, 2012; Hannaford and Marsh, 2006; Lorenzo-Lacruz et al., 2011; Massei et al., 2007; Morán-Tejeda et al., 2011; Wrzesiński and Paluszkiewicz, 2011). Non-stationarity of climate variability has been associated with the North Atlantic Oscillation in most parts of western Europe (Comas-Bru and McDermott, 2014; Harrigan et al., 2014; Massei et al., 2007; Trigo et al., 2004; Vicente-Serrano and López-Moreno, 2008). Moreover, non-stationary modes of climate variability have also been related to the modification of the temporal frequencies and the creation of periodicities in major hydrological variables, including streamflow (Massei et al., 2010) and groundwater levels (Andreo et al., 2006; De Vita et al., 2012; Holman et al., 2011; Neves et al., 2019). Despite growing interest in understanding the drivers of streamflow variability in Western Europe and establishing

* Corresponding author.
E-mail address: jorge.lorenzo@unirioja.es (J. Lorenzo-Lacruz).

https://doi.org/10.1016/j.gloplacha.2022.103797
Received 5 April 2021; Received in revised form 24 March 2022; Accepted 28 March 2022
Available online 5 April 2022

possible connections with general atmospheric mechanisms, there has not been a continent wide study that analyzes the role of these mechanisms on the possible cycles of streamflow in the region. Such an analysis is critical to understanding the temporal and spatial variability of hydrology and to enhance the predictability of streamflow and hydrological drought and flood events (Yuan et al., 2017). This is of particular interest in the region since diverging spatial patterns of floods have been identified, with increasing floods trends in northern Europe and

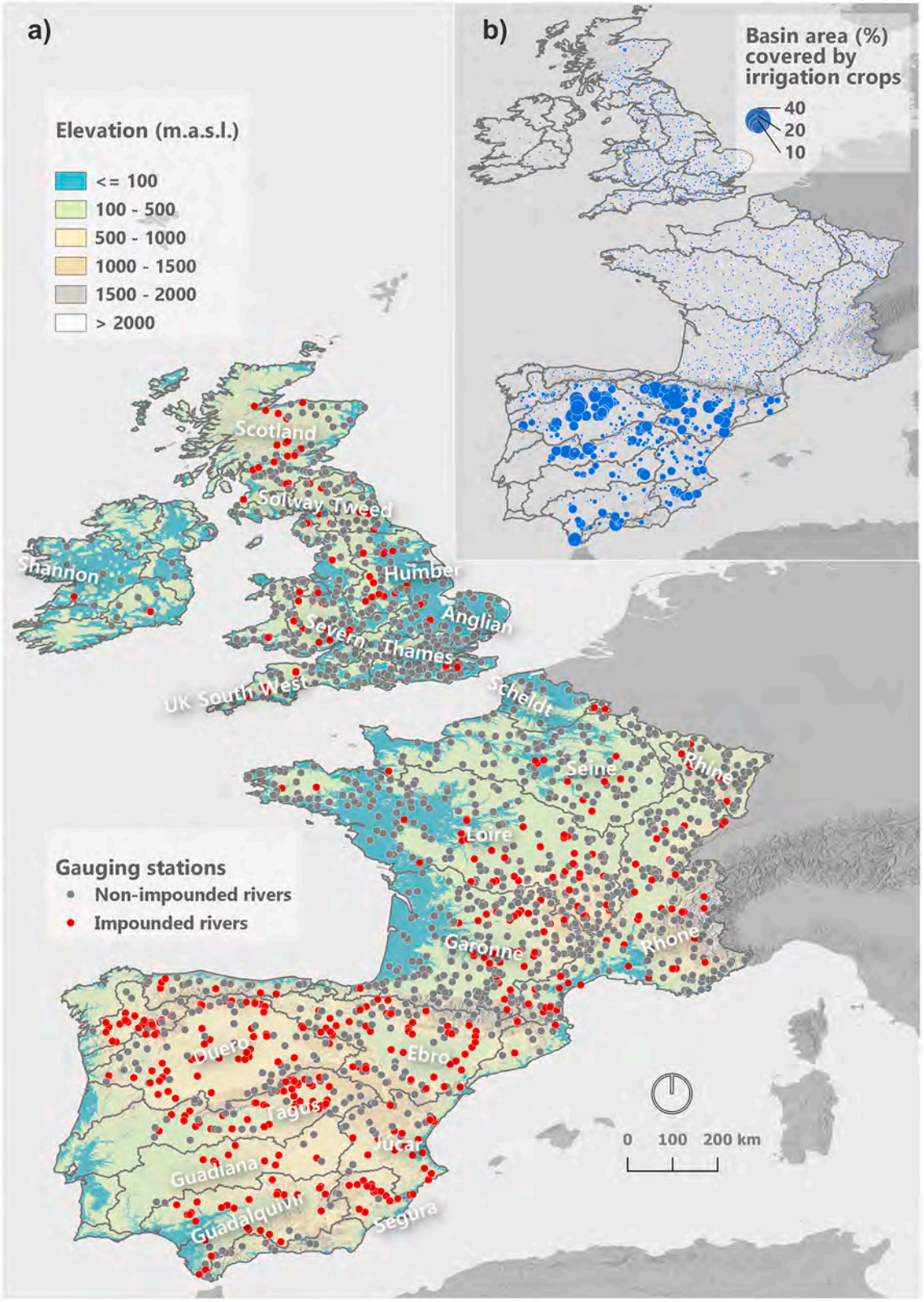

Fig. 1. a) Location of the 1874 gauging stations used in this study, characteristics of the watersheds and main river basins. b) Watershed area covered by irrigation crops.

decreasing trends in the south (Blöschl et al., 2019). Moreover, more frequent and severe hydrological droughts have been identified in southern Europe (Gudmundsson et al., 2017; Lorenzo-Lacruz et al., 2013a), in comparison to less frequent droughts in the rest of the continent (Hisdal et al., 2001; Zaidman et al., 2002).

From a regional perspective, little is known about streamflow frequency dynamics in Europe nor about the effects of coupling with different climate patterns. In this study, we evaluate annual to decadal streamflow periodicities during the last five decades in western Europe (1874 gauging stations; Fig. 1) and study the possible synchronous variability of streamflow with the four most dominant patterns of atmospheric circulation in the region, analysing possible non-stationary relationships between the dominant circulation modes and streamflow. For this purpose, we used the instrumental NAO index (NAOi) from the Climate Research Unit (Gibraltar minus Iceland; https://crudata.uea.ac.uk/cru/data/nao/values.htm), and the EA (EAi), SCAND (SCANDi) and EAWR (EAWRi) monthly indices obtained from NOAA's Climate Prediction Centre (https://www.cpc.ncep.noaa.gov/data/tele

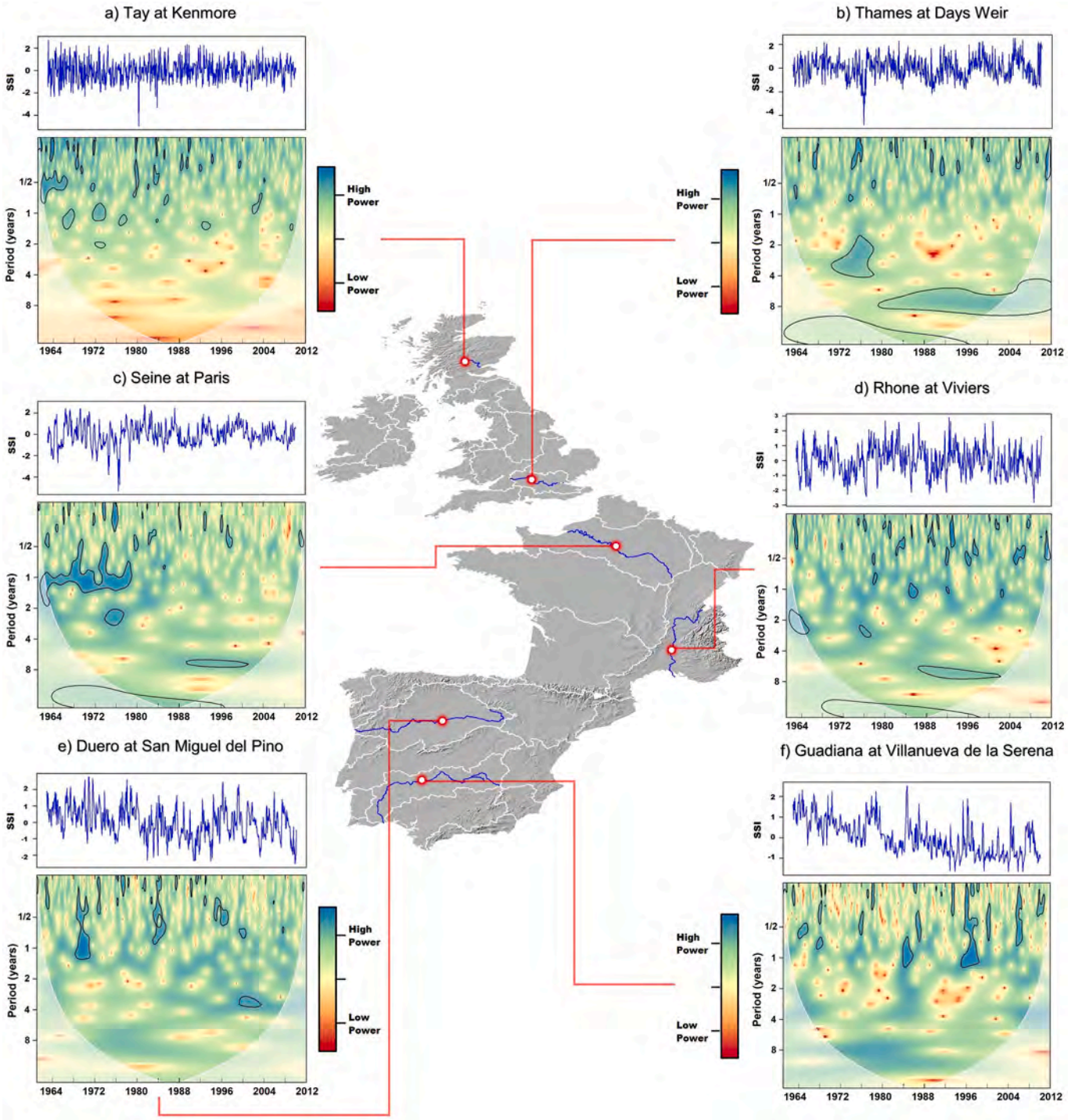

Fig. 2. Continuous Wavelet Transform (CWT) power spectra for selected monthly streamflow series across the study area, and corresponding monthly SSI series. The thick black contour lines enclose regions of confidence levels greater than 95%. The white line depicts the cone of influence (COI), where edge effects may not be negligible.

doc/telecontents.shtml) (Fig. 2), following the approach of Holman et al. (2011). Winter and summer indices were defined as the average monthly value of the climate indices during winter (DJFM) and summer (JJAS) time. To identify possible changes in streamflow frequencies we use wavelet transform analysis (Grinsted et al., 2004; Labat, 2005; Torrence and Compo, 1998) using a monthly streamflow database with high spatial resolution. Our results fill a gap in understanding streamflow frequencies in western Europe, broadening the insights obtained by previous research that has typically focused on the catchment- to regional-scale (Labat, 2008; Massei et al., 2010; Rust et al., 2020).

2. Data set

The streamflow database used in this study was developed using the available monthly streamflow series from the different water management agencies in the countries of Western Europe. The original database comprised a total of 4664 gauging stations characterized by strong spatial density over the region, but showing some temporal differences in data availability. The series with at least 75% of data available for the 1961–2012 period were retained for its reconstruction and gap filling. For each target station (≥75% available data), we selected from the entire dataset, the nearby stations that met three conditions in regard to target station: (1) being located no further than 100 km away, (2) having at least a correlation of $r = 0.7$ and (3) overlapping 7 years of common data. Monthly standardized series were created from each nearby station and target station by calculating empirical cumulative distribution functions. As nearby stations contained also missing data, a reference series was constructed considering the most correlated (Pearson's r) monthly standardized nearby stations with the monthly standardized target series. Finally, gaps from target station were filled with the reference series transformed to original units (hm^3). The final reconstructed data set corresponded to a total of 1874 monthly streamflow series (895 in France, 474 in UK, 472 in Spain, 16 in Portugal and 17 in Ireland), with a common period spanning from 1962 to 2012. Considering the total of 1874 series, 469 (26%) correspond to impounded rivers, and 1405 (74%) correspond to non-impounded rivers. More details about the compilation and validation of this database can be found in (Vicente-Serrano et al., 2019). Monthly streamflow data used in this study can be accessed via https://msed.csic.es/. Fig. 1 shows the spatial distribution of the gauging stations used in this study. Delineation of watersheds corresponding to 1874 gauging stations was performed using ArcHydro tools® and a 25 m resampled DEM provided by the EU Copernicus data and information program.

3. Methods

3.1. Standardization of streamflow series

The use of a robust and flexible method for standardization of streamflow series is a requirement when dealing with large hydrological datasets, to ensure comparability of series across time and space. The use of standardized series is also crucial when using wavelet transforms, since wavelet power at higher frequency periods may be overestimated due to the presence of annual cycles (Agarwal et al., 2016a, 2016b; Grinsted et al., 2004). Here we used the Standardized Streamflow Index (SSI) Vicente-Serrano et al., 2012, which transforms raw monthly streamflow records into standardized anomalies expressed as z-scores (with mean = 0 and standard deviation = 1). The most suitable probability distribution is selected from among six different distributions, providing a versatile approach for the calculation of a streamflow index that ensures the adaptability of the new standardized variable to different climatic and hydrological regimes. Various formulations of the SSI have been successfully used in diverse spatial contexts involving a range of hydrological variables (Barker et al., 2016; Huang et al., 2016; Lorenzo-Lacruz et al., 2017; Peña-Gallardo et al., 2019; Telesca et al., 2012; Vicente-Serrano et al., 2017; Wan et al., 2017). SSI has also already been used for wavelet analysis in various spatial contexts (Huang et al., 2016; Li et al., 2019).

3.2. Continuous Wavelet Transform (CWT)

Wavelet transforms are a popular tool for analysing nonstationary variance in geophysical and ecological series, due to their ability to decompose hydro-climatic series into time-frequency space (Agarwal et al., 2017; Anctil and Coulibaly, 2004; Andreo et al., 2006; Cazelles et al., 2008; Labat, 2010, 2008, 2006; Tamaddun et al., 2017). Basically, a wavelet is a function with zero mean that is localized both in time and space (Farge, 1992), which is used as a consecutive series of band-pass filters applied to the time series (Grinsted et al., 2004).

In this study we used the Morlet wavelet function because it contains real and imaginary parts, allowing the separation of the amplitude and the phase of the signal (Cazelles et al., 2008; Torrence and Compo, 1998), it provides a good definition in the frequency domain compared to commonly used wavelets (Maheswaran and Khosa, 2012), and has similarity with the signal of the environmental time series used (Holman et al., 2011).

The Morlet wavelet is defined as

$$\Psi_0(\eta) = \pi^{-1/4} e^{i\omega_0\eta} e^{-\frac{1}{2}\eta^2}, \quad (1)$$

where ω_0 is dimensionless frequency and η is dimensionless time. We use the Morlet wavelet (with ω_0=6) for feature extraction purposes (Grinsted et al., 2004).

The Continuous Wavelet Transform (CWT) of a discrete set of observations xn is defined as the convolution of xn with a scaled and translated wavelet $\Psi(n)$ that depends on a non-dimensional time parameter η with zero mean and localized in both frequency and time (Torrence and Compo, 1998), and is expressed as

$$W_n(S) = \sum_{n'=0}^{N-1} X_n \Psi^* \left[\frac{(n-n')\delta t}{S}\right], \quad (2)$$

where n is the localized time index, n' is the time variable, S is the wavelet scale, δt is the sampling period, N is the number of points in the time series, and the * indicates the complex conjugate. Varying the wavelet scale S and translating along the localized time index n, it is possible to obtain a picture showing both the amplitude versus the scale and how this amplitude varies with time (Torrence and Compo, 1998).

In order to avoid an artificial and systematic reduction in power at low periods, instead of displaying the result of the wavelet transforms by plotting the wavelet power spectrum ($|W_n(S)|2$) (Torrence and Compo, 1998), we used the bias-corrected power spectrum proposed by (Liu et al., 2007). A Cone of Influence (COI) is plotted to depict important edge effects caused by the non-complete localization of the wavelet in time, which may result in errors at the beginning and end of the wavelet power spectra.

In this study, CWT was used to unveil streamflow periodicities (cycles) on the 1874 monthly streamflow series included in the data set. Calculations were done by means of the 'biwavelet' R package developed by (Gouhier et al., 2016).

3.3. Cross wavelet transform (XWT)

In this study we used Cross Wavelet Transform (XWT) to relate streamflow periodicities to the dynamics of four different atmospheric circulation indices. The expansion into time-frequency space allows the different wavelet transforms to find localized intermittent periodicities within a time series and also to identify periods of common frequency variations and synchronicities between two different time series. Is this ability of decomposing environmental series into signals at different frequencies located in time, what represents a very useful resource for the analysis of nonstationary hydrological processes and mechanisms

(Adamowski and Prokoph, 2014; Benner, 1999; Milly et al., 2008), including streamflow periodicities and the influence of atmospheric circulation mechanisms (Luque-Espinar et al., 2008; Özger et al., 2009; Pekárová and Pekar, 2004; Sadri et al., 2016; Tamaddun et al., 2017; Zhang et al., 2007).

Specifically, the XWT is constructed using two CWTs, and its purpose is to expose common power and relative phase in time-frequency space, being, in a geometric sense, analogous to the covariance between two time series. Torrence and Compo (1998) defined the cross wavelet spectrum of two time series X and Y with W_n^X and W_n^Y as

$$\left|W_n^{XY}(S)\right| = \left|W_n^X(S) \cdot W_n^{*Y}(S)\right|, \tag{3}$$

where W_n^{*Y} is the complex conjugate of W_n^Y. The complex argument of W_n^{XY} can be interpreted as the local relative phase between time series X_j and Y_j. Thus, phase values less (larger) than $\pi/2$ indicates that the two series move in-phase (anti-phase, respectively), while the sign of the phase difference shows which series is the leading one in the relationship (Rösch and Schmidbauer, 2014). Statistical significance is estimated against a red noise model (Torrence and Compo, 1998). The bias-corrected cross wavelet spectra were computed and plotted using the methods described in Veleda et al. (2012). XWT reveals areas with high common power. Nevertheless, it depends on the unit of measurement of the series and may not readily interpretable with regard to the degree of association of the two series (Rösch and Schmidbauer, 2014). Wavelet coherence may remedy this, although it can find significant relationships even though the common power between series is low (Grinsted et al., 2004).

3.4. Wavelet coherence (WTC)

Within wavelet tools and transforms, another useful analysis is to measure how coherent the XWT of two time series is in time-frequency space. For this reason, here we also used the Wavelet Coherence (WTC) to measure the coherence (correlation) between streamflow periodicities and those of the four atmospheric circulation patterns considered. For this purpose, WTC is calculated as the square of the cross-spectrum normalized by the individual power spectra. This gives a quantity between 0 and 1, and measures the cross-correlation between two time series as a function of frequency. Following Torrence and Webster (1999), Grinsted et al. (2004) defined the wavelet coherence between two time series as

$$R_n^2(s) = \frac{\left|S\left(s^{-1}W_n^{XY}(s)\right)\right|2}{S\left(s^{-1}\left|W_n^X(s)\right|^2\right) \cdot S\left(s^{-1}\left|W_n^Y(s)\right|^2\right)}, \tag{4}$$

where (S) is a smoothing operator. This definition closely resembles that of a traditional correlation coefficient, and it is useful to think of the WTC as a localized correlation coefficient in time frequency space (Grinsted et al., 2004). Statistical significance level of the WTC is estimated using Monte Carlo methods. For more details on the calculation of the statistical significance of the WTC see Grinsted et al. (2004) and Torrence and Compo (1998).

In the present study, we explored the ability of both the WTC and the XWT to identify synoncroniticities between the frequencies observed in streamflow series and the frequencies of the four main atmospheric circulation mechanisms affecting the climate variability in West Europe.

3.5. Streamflow frequency-based regionalization

Based on our large and spatially dense set of observations, we tackle an unprecedented streamflow time-frequency based regionalization for Western Europe by means of Principal Component Analysis (PCA). PCA in S mode (Richman, 1986) was applied to the 1874 power spectra decomposed matrices resulting from the CWT analysis, as well as for those generated by XWT and WTC analysis, so three different PCA were applied. In S mode, the variables from which to compute the Principal Components are the power spectra series derived from each wavelet analysis corresponding to each hydrological station. In this way the principal components summarize groups of stations with a similar temporal signal in the power spectra. The data (CWT/XWT/WTC power spectra) were structured in a matrix with 612 (months from 1962 to 2012) columns by 81 (periods/frequencies in logarithmic scale) rows per site (1874 in total), which constitutes the periodogram calculated by means of each wavelet analysis.

In order to ease the interpretation of the results, a total of 3 principal components were selected for the CWT analysis, which together accounted for a 50% of the total variance (from the 4th principal component onwards, the explained variance was less than 3%). For the XWT and WTC analysis, the number of components retained was also three, which in most cases together accounted for more than 50% of the variance. From the different PCAs we retrieved the factorial scores, which represent the linear combinations of the original variables; as well as the loading factors (coefficients of the linear combinations), that allowed us identify which PCA correlates better with each of the original variables. For regionalization (classification) purposes, we followed the maximum loading rule, in which each catchment (defined by an individual gauging station) was assigned to the Principal Component (PC) that showed the highest loading (Revelle, 2021).

3.6. Atmospheric circulation mechanisms

Numerous studies have shown a substantial influence of atmospheric circulation modes in the North Atlantic region [i.e., the North Atlantic Oscillation (NAO), East Atlantic Pattern (EA), Scandinavian Pattern (SCAND), and the East Atlantic/Western Russia pattern (EAWR)] on hydroclimatic variables, including: precipitation (Comas-Bru and McDermott, 2014; García-Herrera et al., 2007; Hannaford et al., 2011; Kalimeris et al., 2017; Vicente-Serrano et al., 2014; Vicente-Serrano et al., 2016); streamflow (Lorenzo-Lacruz et al., 2011; Steirou et al., 2017); lake levels (Hernández et al., 2015); and groundwater levels (Holman et al., 2011; Neves et al., 2019; Slimani et al., 2009).

The NAO is the dominant climate pattern in the North Atlantic sector and represents a dipole of the pressure field between Iceland and the Azores archipelago. During its positive phases, high pressures are established over the Azores and low pressures centres over Iceland, favouring warmer and wetter winters across northern Europe, and drier conditions in the southern regions of the continent. The influence of the NAO on precipitation and river discharge has been well documented in the western European region (Hurrell et al., 2003; Hurrell and Van Loon, 1997; Trigo et al., 2002), including the British Isles (Burt and Howden, 2013; Wilby, 2001), Ireland (Kiely, 1999), France (Massei et al., 2010, 2007), and the Iberian Peninsula (Lorenzo-Lacruz et al., 2011; Trigo et al., 2004; Vicente-Serrano et al., 2011a, 2011b). While the NAO is a simple dipole index, in a wide continental context its hydro-climatic influence is very variable in its timing, extent, intensity and sign (Moore et al., 2013; Vicente-Serrano and López-Moreno, 2008).

The EA is the second prominent mode of pressure variability over the North Atlantic and it has a dipole configuration similar to the NAO but displaced southeastwards (Barnston and Livezey, 1987; Comas-Bru and McDermott, 2014). During EA positive phases, low pressure centres and associated negative sea level pressures (SLP) are located in the eastern North Atlantic, westwards of the British Islands, generating above-average precipitation over the northern European region and Scandinavia and below-average precipitation across southern Europe. Please note that here we used the convention (of EA phases notation) that a positive EA index reflects more negative SLP conditions in the eastern North Atlantic (and therefore wetter winters in Ireland and the UK), following Moore et al. (2013).

The SCAND pattern was first defined by Barnston and Livezey (1987) as the Eurasia-1 pattern, and shows a principal action centre located over the Scandinavian Peninsula. SCAND positive phases generate

blocking situations over northern Europe, leading to above-average precipitation across central and southern Europe, and below-average precipitation across Scandinavia. EA has an intense interaction with the SCAND pattern, and sometimes the EA eastwards shifting and the SCAN southwestwards shifting, creates a kind of a blend of both patterns (Barnston and Livezey, 1987). Moreover, Comas-Bru and McDermott (2014) showed how EA and SCAND patters modulate the influence of NAO by changing the positions of the NAO dipole.

The EAWR is the last of the four patterns considered affecting Eurasian climate. It was first referred to as the Eurasia-2 pattern (Barnston and Livezey, 1987), and consist of four main anomaly centres. Those pressure centres affecting the Western European climate are located over northern Europe (positive height anomalies) and over the Central North Atlantic Ocean (negative height anomalies). Positive phases of this pattern favour below-average precipitation across central Europe (Krichak and Alpert, 2005).

4. Results

Fig. 2 shows an example of the CWT analysis applied to six SSI representative series distributed across the study area. The CWT power spectra for the Tay river at Kenmore, Scotland (Fig. 2a) is characterized by alternating strong fluctuations (high power patches in the periodogram) around the ½- and 1-year frequency periods (bi-modal and uni-modal discharge regimes) during the whole study period, and by the absence of significant cycles at low frequency periods (>1 year).

The Thames at Days Weir (Fig. 2b) shows a clear change in its CWT periodogram: during the 1970s, discharge exhibited high power at the 2 and 3-years periods; since then, a high power band is stablished around the 7-years period, lasting until the end of the record. Despite the last part of this high power band falling outside the COI, the CWT shows a systematic cycle of high-low discharges every 7 years. Streamflow frequencies in the Seine river at Paris (Fig. 2c) also show important changes. During the 1960s and 1970s the CWT exhibited a marked band

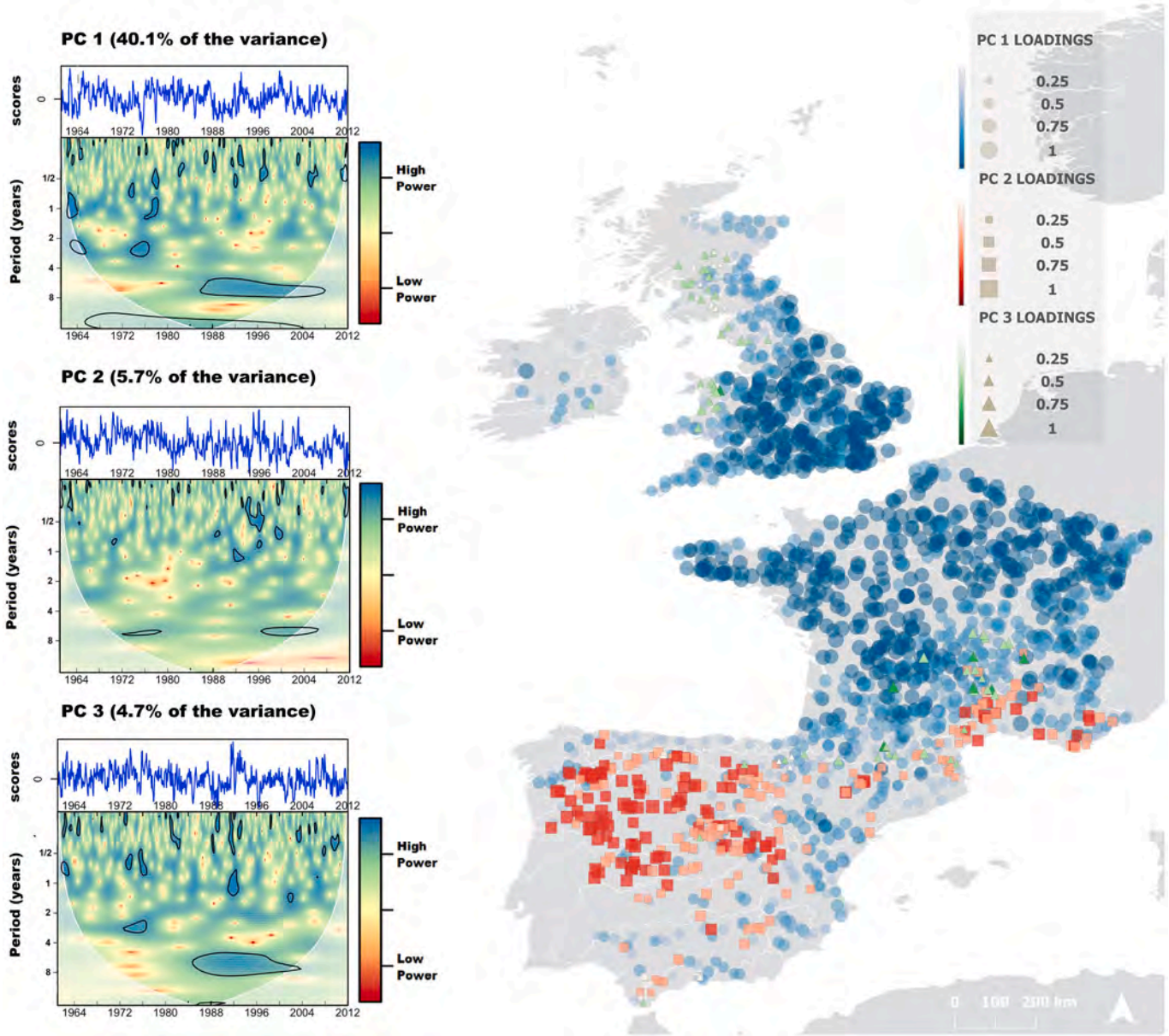

Fig. 3. Left panels: Continuous Wavelet Transform (CWT) power spectrum of the three selected Principal Components and corresponding SSI series; right panel: spatial distribution of the loadings between decomposed wavelet scores of selected Principal Component and individual wavelet scores derived from SSI series (only stations showing highest loading with this particular PC are shown).

of high power around the 1-year period, whereas a significant band of high power appeared around the 7-years period, between 1988 and 2000. Similar changes are also evident for the Rhone river at Viviers (Fig. 2d): CWT changed from sparse patches of high power around 2-years period during the 1960's and 1970's, towards a band of high power around the 7-years between 1987 and 2003. In this case, a reinforcement of high power at short periods (around ½-year) was observable during the second half of the study period. CWT of selected river discharges in the Iberian Peninsula rarely shows high power at time periods larger than 1 year. The Duero river discharge (Fig. 2e) showed three patches of high power between the ½- and 1–year period in 1970, 1984 and 1996. Similarly, the Guadiana river discharges CWT show high power around the ½-year periods (Fig. 2f), although during the second half of the study period additional power patches appear around the 1-year period (1984–85, 1996–97). Intense river regulation, mainly for irrigation, may be responsible for these frequency configurations: the release of water to meet irrigation demand during particular months of the year (May–October) generates a continuous succession of high frequency flows (including an artificial ½-year frequency period) created by the releasing of water during summer to meet the demand, thus increasing CWT power at shorter time periods.

4.1. Observed changes in streamflow frequencies and persistence of recent low frequency fluctuations

Fig. 3 shows the characteristic CWT power spectra for the three selected PCs and the corresponding SSI series (right panels), and the spatial distribution of the loadings between decomposed wavelet scores of each PC and individual wavelet scores derived from each one of the SSI series. For ease of interpretation, we only show, in each case, the stations with the highest loading for each particular PC, following the maximum loading rule. The regionalization process by means of a PCA achieved coherent spatial patterns.

PC1 accounts for 40.1% of the total variance. Time-frequency dynamics of river discharges related to PC1 are characterized by a CWT spectrum encompassing several patches of high power at periods around 1-year until 1980 and a significant patch of power around the 3-years period between 1973 and 1977. From 1984 to 2012, PC1 exhibits a great change in streamflow frequencies, observable in a band of high power around the 7-years period, accompanied by high power patches around the ½-year period. The hydrological change experienced by catchments related to PC1 can be summarized as the substitution of high intra-annual streamflow variability during the decades of 1960, 1970 and the first half of 1980 (mean around the 1-year period), by more marked low frequency dynamics structured around the 7-years (period) cycle. Spatially, this pattern is centred around the English Channel, with a gradient in the magnitude of the loadings: the closer to the English Channel, the higher loadings that were recorded, encompassing the Thames, South-western, Anglian and Severn river basins in Britain, and the lower and medium reaches of the Loire, Seine, Garonne and Scheldt river basins in France.

PC2 explains 5.7% of the variance. Discharge series associated with PC2 only showed a significant power patch around the 7-years frequency during the first half of the study period. However, during the second half, abundant significant power patches can be observed at shorter frequencies, and the band depicting the 7-years cycle became significant only between 1996 and 2007. Catchments showing highest loadings with the PC2 are located in the Minho, Duero and Tagus basins in the Iberian Peninsula, and in the lower reaches of the Rhone basin, spreading along the Mediterranean coast of France.

PC3 (4.7% of the variance) CWT spectrum shows a similar shape to the one observed for PC1, with two contrasted periods, before and after 1980, in which streamflow frequencies showed notable differences. Before 1980, significant periodicities can only be observed at short and mid frequency periods (<1–year and 3-years). From 1980 onwards, significant power patches can be still observed at high frequency periods, although the most relevant feature is, again, the observation of a great band of significant power around the 7-years cycle. Gauging stations related to PC3 spread across western England and Wales, the Massif Central and the Pyrenees.

The analysis performed in this section reveals a hydrological change that took place across most of the study area: the substitution of the two main river discharge cycles (identified at frequencies of 1- and 3-years periods), observed until the decade of 1980, by two other cycles detected around the frequencies of ½-years (annual bimodal discharge peak) and around the 7-years period.

4.2. Non-stationarity of North Atlantic climate patterns

The CWT of the NAO reveals the non-stationary behaviour of this climate mode (Fig. 4a), showing a clear strengthening of the NAO signal since the middle of the 1980s (increased power at the 1-year frequency period). During the 1960s and 1970s, significant power patches can rarely be found, and always at short frequencies (< 1-year). From 1985 onwards, numerous significant power patches appear at short time frequencies, around the ½- and 1–year periods; in addition, two significant patches were observed at longer time frequencies, around 7-years between 1987 and 1992, and around 2-years at the end of the series.

The CWT of the EA monthly index (Fig. 4b) shows oscillations between the ¼- and ½-years during the whole study period (1962–2012). Long-term fluctuations of the EA are located around 4-years periods during the 1970s, although sparse significant power patches around 2-years can be found in the 1960s, 1990s and 2000s. The CWT spectrum of the SCAND monthly index (Fig. 4c) shows a very active phase of this pattern during the 1980s and the first half of the 1990s. During this period, the SCAND pattern exhibited strong fluctuations at short (1-year) and long (around 7-years) periods. From 2000 onwards, patches of high power at frequencies greater than 4 months are no longer present suggesting a weakening of the SCAND pattern. The CWT spectrum of the EAWR pattern showed two active phases (Fig. 4d): in the first one, during the 1960s and 1970s, the pattern experienced strong fluctuations at short periods (½- and 1-year); in the second one, during the 1980s, significant power patches appeared at the 2-years and the 7-years periods. Since 2000, the pattern has weakened and significant periodicities disappeared.

4.3. Changes in SSI periodicity and the role of atmospheric circulation mechanisms

Next we explore how the dominant atmospheric circulation mechanisms that affect the climate in the North Atlantic region may determine or influence changes in streamflow periodicities. We divide this section into different subsections devoted to each of the main circulation mechanisms indicated above: NAO, EA, SCAND, and EAWR. The results include the influence of these climate patterns on changes detected on the frequencies of SSI series by means of the Wavelet Coherence analysis, and the changing influence of each circulation mechanism on the SSI between two contrasted periods (first half, 1962–1986, and second half,1987–2012), illustrated with correlation coefficients.

4.3.1. North Atlantic Oscillation

Fig. 5 shows the WTC power spectra between the NAO index and the SSI series summarized by the first three PCs (53% of the variance). Phase values (arrows in the periodograms) less (larger) than $\pi/2$ indicates that the two series move in-phase (anti-phase, respectively), while the sign of the phase difference shows which series is the leading one in the relationship. The periodograms of PC1 (41%) and PC3 (5%) show similar features. Significant cycles are common around 3-years during the 1960s and 1970s can be observed in PC1 and PC3. However, upwards left pointing arrows within these patches depict an anti-phase relationship, denoting negative correlations between the NAO and the SSI series during the first part of the study period. From the 1990s onwards, a

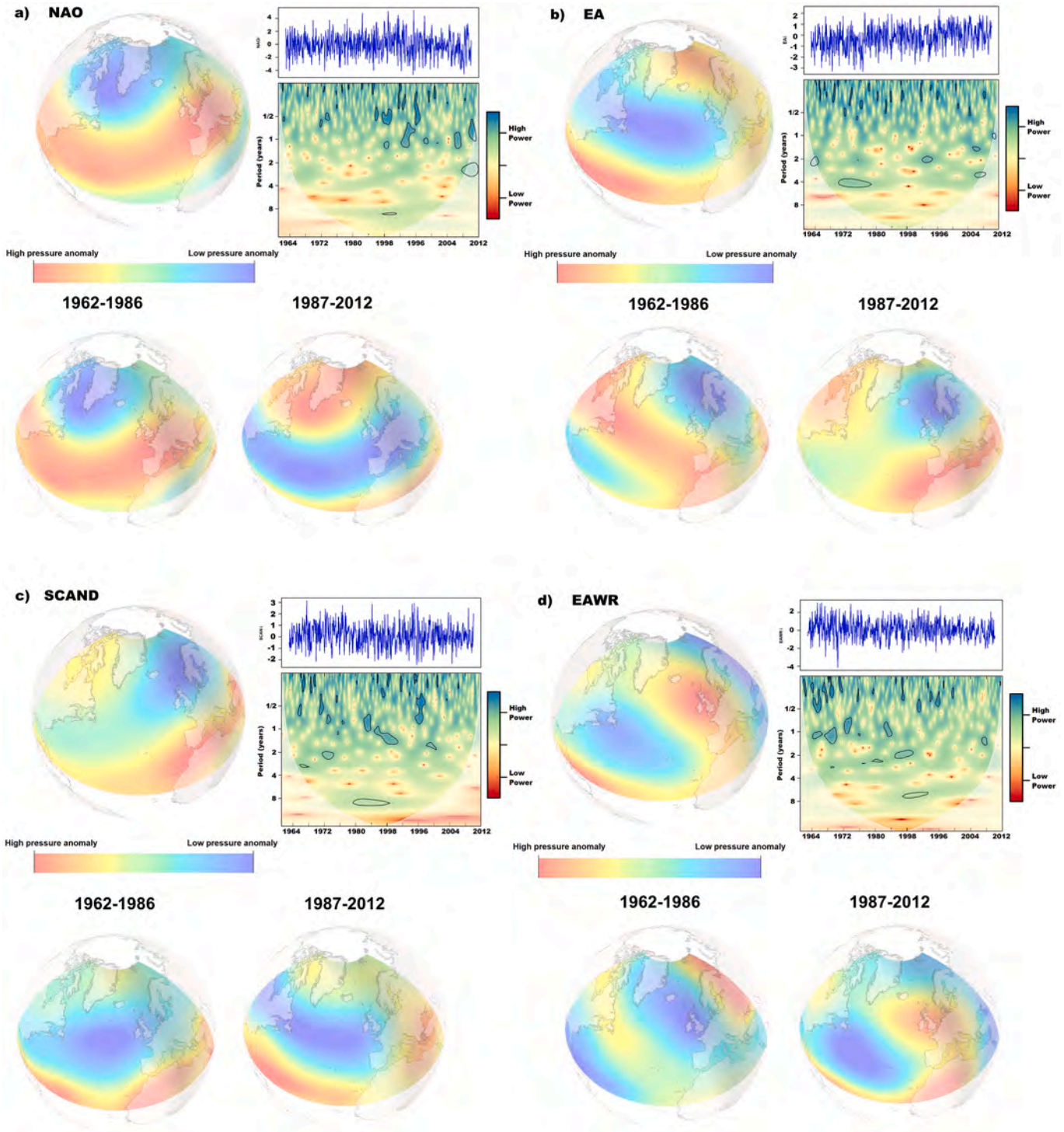

Fig. 4. (a) NAO, (b) EA, (c) SCAND and EAWR (d) patterns. Upper globes: spatial patterns of the corresponding empirical orthogonal function of the 500 hPa geopotential height over the North Atlantic sector during winter time (DJFM). Upper right panels: climate pattern indices and derived CWT. Lower left globes: spatial patterns of the corresponding orthogonal functions of the 500 hPa geopotential height over the North Atlantic sector during winter time (DJFM) for the period 1962–1986; lower right globes: same for the period 1987–2012.

significant band of coherence around the 7-years period is clearly identified for PC1 and PC3. However, within these bands of high common power, right pointing arrows (less than $\pi/2$) depict in-phase relationships; therefore, only the diagonal downward right pointing arrows appearing from 1992, indicate some degree of lead between the NAO signal and the 7-years periodicity detected in the SSI series. This means that the explanatory potential of the NAO regarding the 7-years cycle is limited to the last two or three decades of the study period. The verticality of the arrows within these patches denotes an important lag between the NAOi and the SSI series. Moreover, the change from anti-phase to in-phase interactions between the NAO and the SSI series related to PC1 is corroborated by the change of the sign of the correlations between winter NAOi and SSI series observed in most parts of Britain (Fig. 5c and d): correlations in this area changed from significant

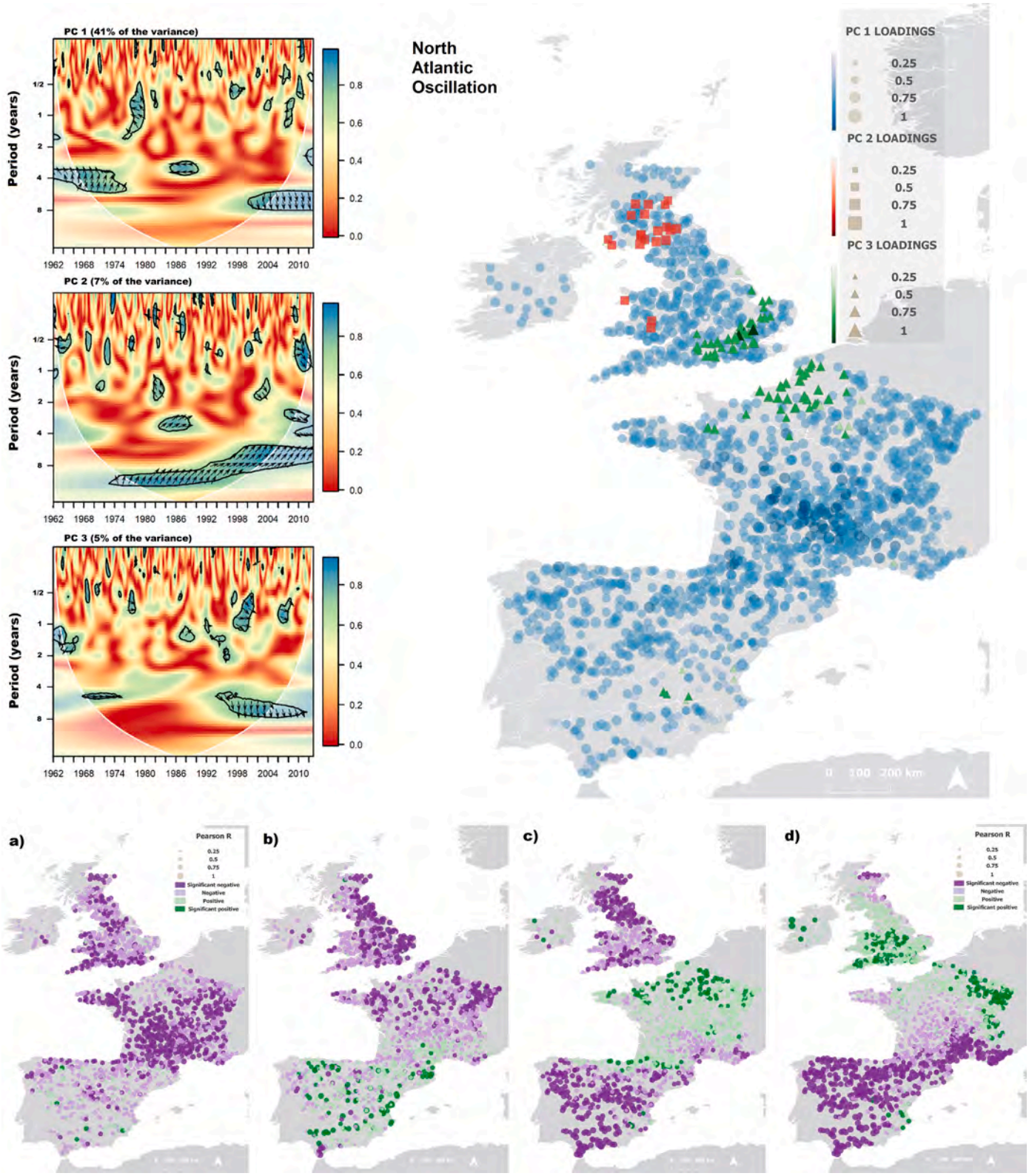

Fig. 5. Summary of the influence of the NAO pattern on streamflow frequency changes across the study area. Left upper panels: Wavelet Coherence (WTC) power spectra between the NAO index and individual SSI series summarized by the three selected Principal Components. Right upper panel: spatial distribution of the loadings of the decomposed Wavelet Coherence scores between the SSI series and the NAO index. Lower panels: a) correlation coefficients between the NAO summer index and SSI series between 1962 and 1986; b) same between 1987 and 2012; c) correlation coefficients between the NAO winter index and SSI series between 1962 and 1986; d) same between 1987 and 2012.

negative between 1962 and 1986, to significant positive from 1987 to 2012. Regarding PC2 (7% of the variance), diagonal upward right pointing arrows contained in the band of coherence at low frequency periods denote a lead of the SSI series in the interaction with the NAO. Although both signals are in-phase, this incongruity will not be considered for discussion, since it is not a coherent physical mechanism that streamflows lead the relationship with the NAO.

PC1 spreads across the whole study area, with higher loadings in the central and southern British basins (including the Tweed, Humber, Severn, Anglian and Thames basins), and the upper and middle reaches of the Seine, Loire and Garonne basins. PC2 corresponds to basins located in Wales and the north of England. PC3, with very similar (enhanced) features compared to PC1, is related to English and French catchments flowing into the English Channel. Fig. 4a shows the different spatial (averaged) patterns adopted by the NAO pattern during two contrasted periods. During the first half of the study period (1962–1986), winter low pressure anomalies were centred over Greenland and Iceland, whereas predominant high pressure anomalies covered most of central and southern Europe. During the second half of the studied period (1986–2012) low pressure anomalies predominate over central and southern Europe and high pressure over Greenland and Iceland. This results in the northwards displacement of significant correlations between the NAO winter index and SSI series during the second half of the study time span, together with a strengthening of the magnitude of negative correlations in the Iberian Peninsula and south-eastern France between 1986 and 2012. Significant negative correlations are also evident in northern Spain, the French Pyrenees, the lower reaches of the Rhone basin and small catchments flowing into the Côte d'Azur. Moreover, the significant positive correlations observed in northern France during the first half of the study period, are common north-eastwards and spread (increasing in number) along south England and Wales, and eastern France between 1986 and 2012. The significant negative correlations during winter in the UK were restricted to small areas in eastern Scotland. Also noteworthy are the increasing number of positive correlations between the NAO summer index and SSI series in the Iberian Peninsula during the second half of the study period. These results suggest that the reinforcement of the NAO signal, and the associated predominance of positive correlations in England and France during recent decades is likely related to the appearance (since the mid 1980s) of the 7-years SSI periodicity detected in previous sections.

4.3.2. East Atlantic pattern

Fig. 6 shows the WTC power spectra between the EA index and the SSI series summarized by the first three PCs (46% of the variance). Short-term interactions (¼- and ½-years frequency periods) between the EA and the SSI are observed over the whole study period, in the case of the first three PCs. Regarding PC1 and PC2, the influence of the EA on long-term streamflow fluctuations is only significant between 1962 and 1975, at a periodicity of 2-years. Right pointing arrows within these patches denote in-phase relationships between the EA and SSI. Nevertheless, since 1980 long-term interactions between EA and SSI are not recorded in almost the entire study area (the exception is PC3). This would suggest decreasing influence of the EA pattern in the SSI periodicity. XWT analysis (Fig. 9) confirms these results with patches of significant covariance between the EA pattern and the SSI series only observed in the decades of 1960 and 1970 with 2- and 6-year cycles.

A decreasing influence of the EA is recorded in France. Regarding EA influence during winter, several changes were found. During the first half of the study period, significant positive correlations were observable across the whole study area (Fig. 6c), especially in France ($R > 0.7$). On the contrary, between 1987 and 2012, significant correlations can no longer be found in central and southern France (Fig. 6d). Moreover, an important change in the sign of the correlation during winter (from significant positive to significant negative) occurred in most catchments in England, Wales and Scotland. It is noteworthy that this region roughly corresponds with PC2 (characterized by the absence of significant coherence at low frequency periods during the second half of the study span), reinforcing the idea of the decreasing importance of the EA in explaining low SSI frequencies. The decreasing number of significant correlations found between the EA pattern and the SSI series during summer, considering both periods (Fig. 5a and b), supports this idea. These changes may be related to the shifts experienced by the EA pattern and its coupling with the NAO (Fig. 4b).

4.3.3. Scandinavian pattern

Considering the interactions with the Scandinavian pattern, Fig. 7 highlights stationarity in the WTC spectra of the first three PCs during the study period. The interaction at high frequency periods is sustained during the whole study span considering the three retained PCs (51% of the explained variance), with abundant significant coherence patches being observable at the ½- and 1-year periods.

In the case of PC1 (the dominant component spreading across the whole study area), in-phase interactions between SSI series and atmospheric circulation, with the SCAND pattern leading them, can be observed between 1984 and 1990 and between 2000 and 2005 around the 2-years period, with small lags between the SCAND pattern and river discharges. In the case of PC2 and PC3, regions of high coherence are also observed during the same periods, but the interactions in these cases are in anti-phase, with the SCAND pattern leading the relationship (upwards left pointing arrows). This is consistent with the changes in the correlations between the SCAND winter index and SSI series for those catchments corresponding to PC2 and PC3 (Fig. 7c and d). Many SSI series in Wales and England show a change in the sign of correlations during winter with the SCAND pattern, from positive to negative. This is the major noticeable change in the SCAND-SSI interaction dynamics, since, unlike other major climate patterns, the spatial configuration of the SCAND pattern remained similar during both study periods (Fig. 4c and Fig. 7). Even so, significant positive correlations were dominant during winter in southern France and the northern Iberian Peninsula between 1987 and 2012, in comparison to the correlations identified during the first half of the study period. It is also important to highlight the decreasing number of significant correlations recorded during summer between the SCAND pattern and the SSI series. This may explain why the contribution of the SCAND pattern in explaining the generalized 7-year cycle found in streamflows is restricted to the decade of 1980 and 1990.

4.3.4. East Atlantic Western Russia pattern

Fig. 8 shows the interactions between streamflow frequencies and the EAWR pattern as depicted by the WTC analysis for the first three PCs. The dynamics of high frequency fluctuations (½- and 1-year periods) of the three PCs are similar, although a large number of significant coherence patches are observable in the case of PC1. The most significant feature regarding low frequency periods is the band of coherence (of varying size) at the 7-years period that can be observed during the 1980s in the case of PC1 and PC3. This is consistent with the increasing influence of the EAWR on streamflow during winter shown by the means of correlations in Fig. 8c and d, and by means of the XWT analysis shown in Fig. 9.

The spatial configuration of the EAWR pattern (Fig. 4d) experienced a clear change in the location of the associated pressure centres, with the migration of the low pressure centres located over the British and Irish Isles (dominant pattern during the 1962–1986 period) towards the centre of the Atlantic Ocean and the location over the British and Irish Isles of high pressure centres between 1987 and 2012. As a result, significant negative correlations between the EAWR and individual SSI series during winter time, that were only observed in the upper reaches of the Loire and Garonne basins during the first half of the study period, spread across most of France during the second half (Fig. 8c and d). In addition, significant negative correlations appeared in the Spanish Mediterranean basin between 1987 and 2012. Significant correlations between the SCAND summer index and SSI series decreased in number

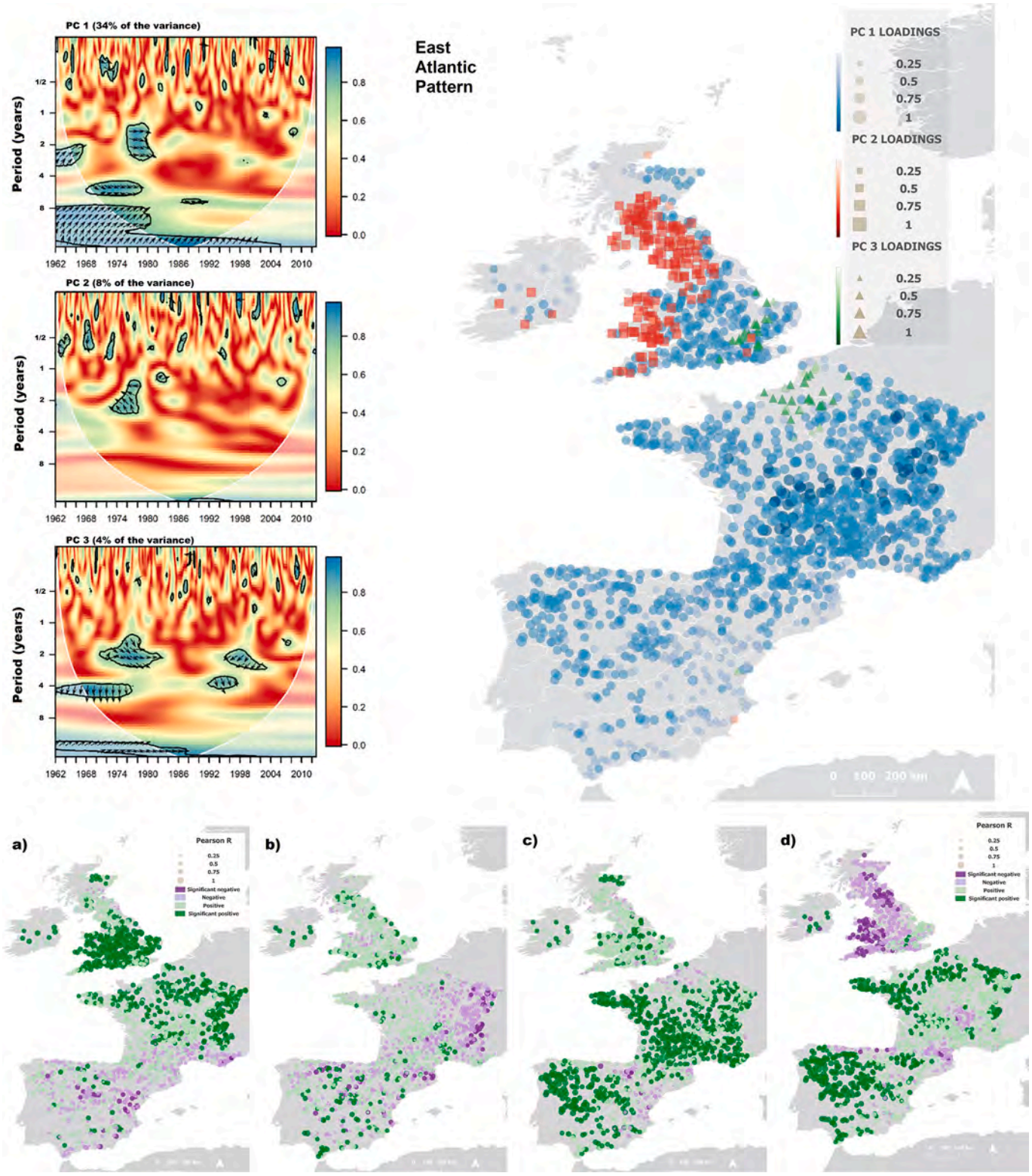

Fig. 6. Summary of the influence of the EA pattern on streamflow frequency changes across the study area. Left upper panels: Wavelet Coherence (WTC) power spectra between the EA index and individual SSI series summarized by the three selected Principal Components. Right upper panel: spatial distribution of the loadings of the decomposed Wavelet Coherence scores between the SSI series and the EA index. Lower panels: a) correlation coefficients between the EA summer index and SSI series between 1962 and 1986; b) same between 1987 and 2012; c) correlation coefficients between the EA winter index and SSI series between 1962 and 1986; d) same between 1987 and 2012.

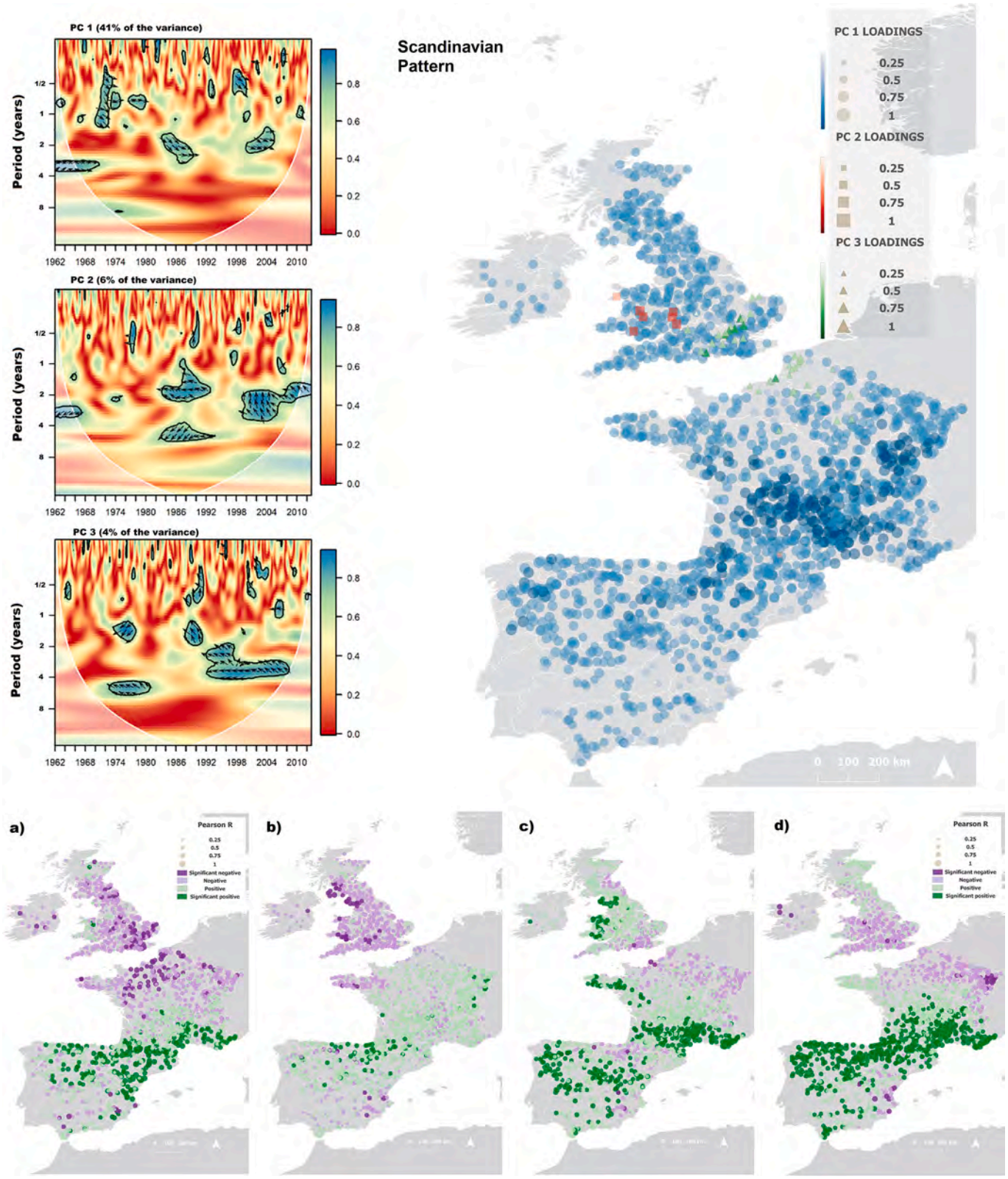

Fig. 7. Summary of the influence of the SCAND pattern on streamflow frequency changes across the study area. Left upper panels: Wavelet Coherence (WTC) power spectra between the SCAND index and individual SSI series summarized by the three selected Principal Components. Right upper panel: spatial distribution of the loadings of the decomposed Wavelet Coherence scores between the SSI series and the SCAND index. Lower panels: a) correlation coefficients between the SCAND summer index and individual SSI series between 1962 and 1986; b) same between 1987 and 2012; c) correlation coefficients between the SCAND winter index and individual SSI series between 1962 and 1986; d) same between 1987 and 2012.

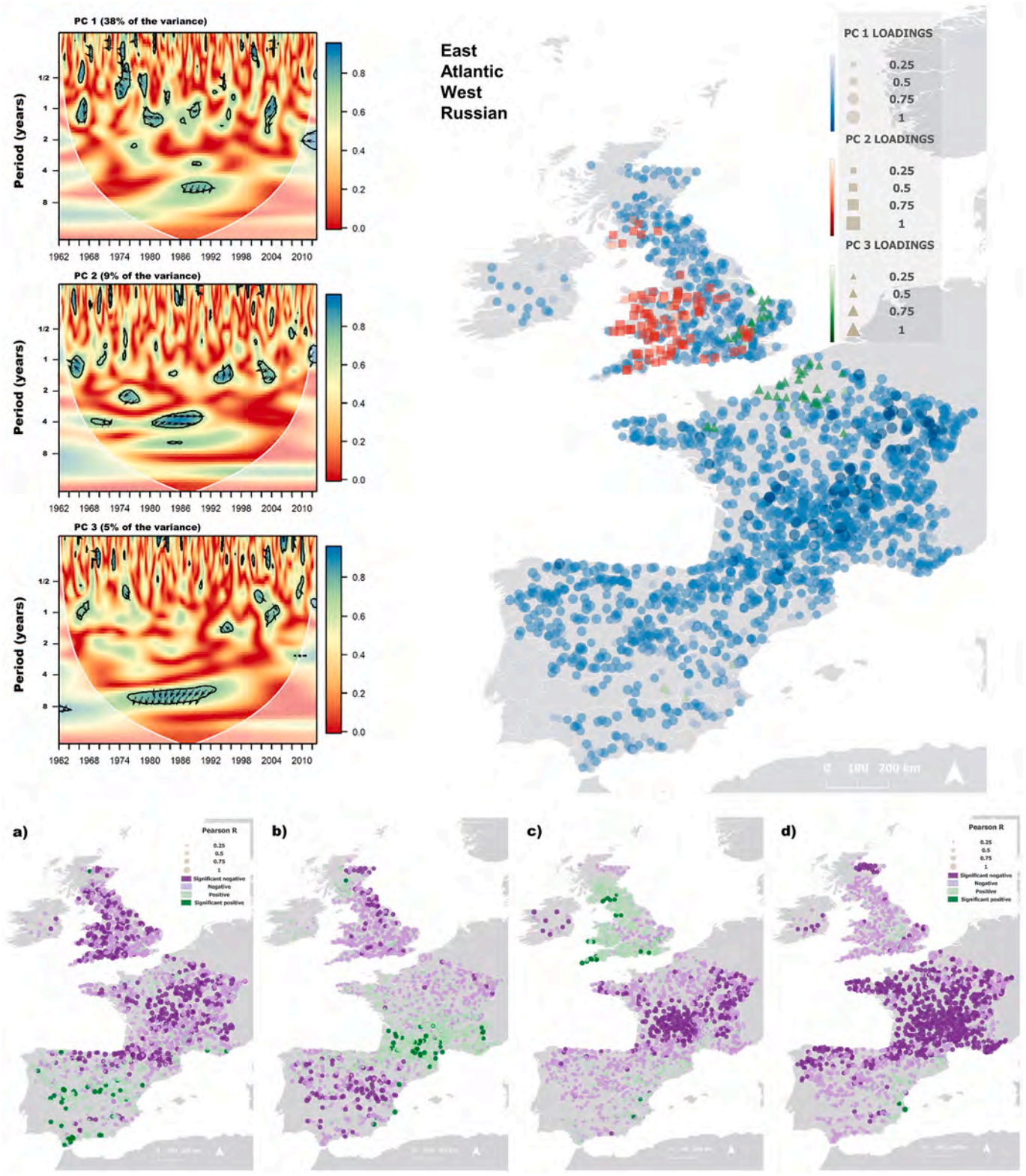

Fig. 8. Summary of the influence of the EAWR pattern on streamflow frequency changes across the study area. Left upper panels: Wavelet Coherence (WTC) power spectra between the EAWR index and individual SSI series summarized by the three selected Principal Components. Right upper panel: spatial distribution of the loadings of the decomposed Wavelet Coherence scores between the SSI series and the EAWR index. Lower panels: a) correlation coefficients between the EAWR summer index and SSI series between 1962 and 1986; b) same between 1987 and 2012; c) correlation coefficients between the EAWR winter index and individual SSI series between 1962 and 1986; d) same between 1987 and 2012.

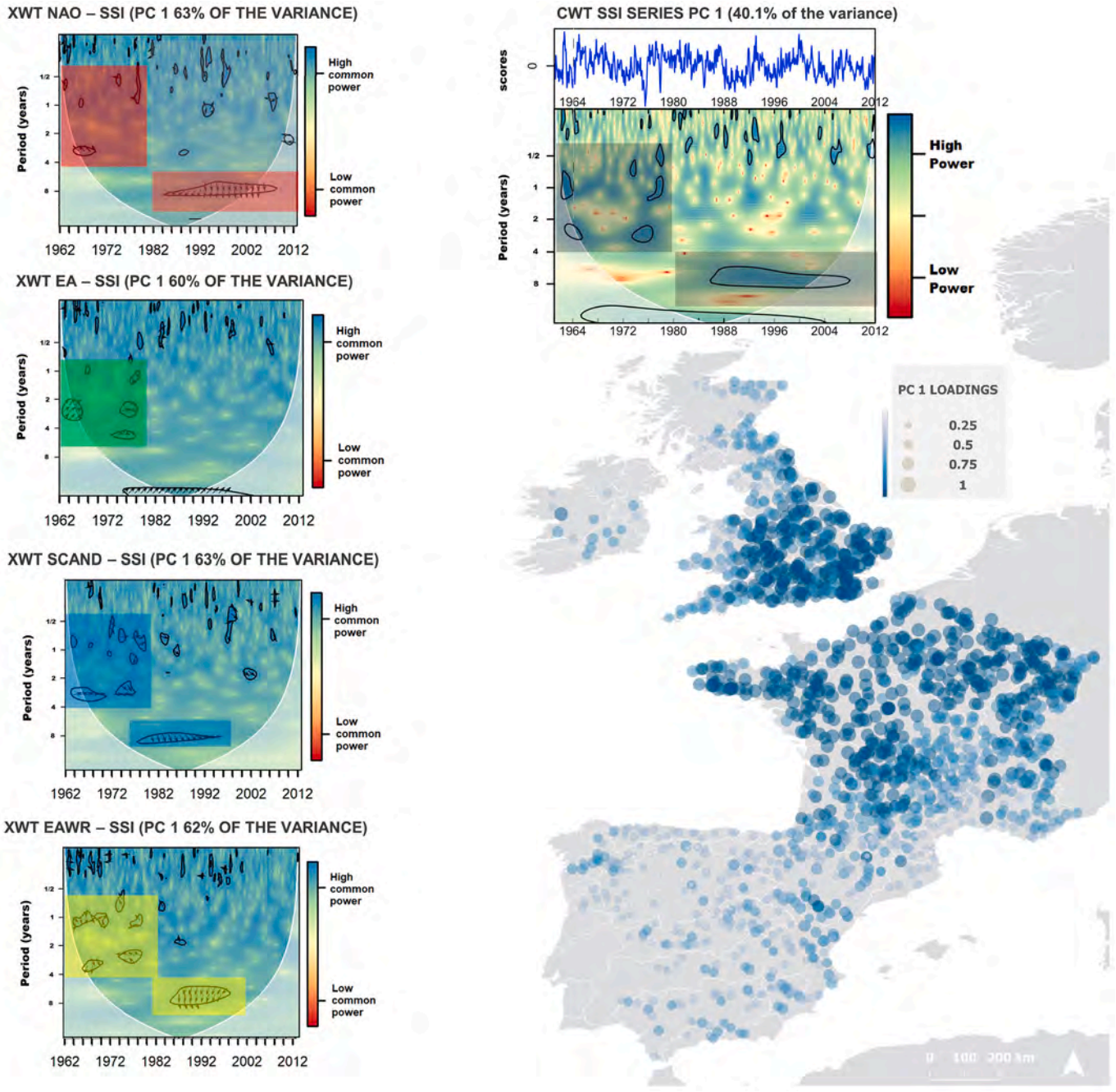

Fig. 9. Summary of changes in streamflow frequencies favoured by the transitive coupling of the four climate patterns, exemplified by the main regional pattern (PC1). Left panel: Cross Wavelet Transforms (XWT) between SSI series and the NAO, EA, SCAND and EAWR patterns. Right panel: PC1 CWT and spatial distribution of the loadings between PC1 scores and individual CWTs at each gauging station.

during the second half of the study period, especially in UK and France (Fig. 8a and b). Also in summer, the significant positive correlations between the EAWR and streamflow in central and southern Iberia evident between 1962 and 1986, moved northwards, being recorded in the south of France between 1987 and 2012. The difference in the locations of the pressure centres of the EAWR index between the two time periods may explain the changes in streamflow relationships.

4.3.5. Climate patterns transitive coupling

The very complex interactions and synchronicities found between the frequencies of the four atmospheric circulation mechanisms and those of the 1874 river basins analysed by means of the Wavelet Coherence and Cross Wavelet Analysis (XWT) revealed common pattern in the changes experienced for mid and low frequency fluctuations. This is illustrated in Fig. 9, where the first retained PC for each of the four XWT analyses performed (SSI against NAO, EA, SCAND and EAWR) are shown together for comparison purposes (left panel). In addition, the regional changes on streamflow frequencies summarized by the first PC (40% of the variance) of the CWT analysis are shown (right panel). Dominant cycles of intense interaction between streamflow in Wales, England and France, and the four analysed climate patterns were observed at periods shorter than three years during the 1960s and 1970s. The coupled influence of all considered climate patterns during these decades may partially explain the main frequencies observed in streamflow, which were also detected at frequencies shorter than 3 years.

A significant regional change in streamflow fluctuations occurred in the mid 1980s, and a consistent pattern of succession of high and low discharge periods every 7-years was stablished during the last 30 years in most parts of the study area, with greater intensity and persistence close to the English Channel. Afterwards, the role of the EA decreased in importance, whereas the influence of the SCAND and EAWR were restricted to the 1980s and 1990s. Since the mid of the 1980s, the NAO showed significant long term synchronicities with the SSI regarding the XWT, with an increasing importance of the NAO influence on streamflow variability, and more specifically, in the persistence of the observed 7-years cycle until the end of the study period. The spatial extent of this change is highly relevant with our CWT analysis indicating that PC1 and PC3 (50% of the variance) experienced of the establishment of high and low discharge cycles every 7 years since the 1980s.

5. Discussion

In this study we have analysed the dynamics of western European streamflow in the time-frequency domain, revealing important changes in periodicities and cycles, that are closely related to changes in the influence of the main atmospheric circulation mechanisms that affect the climate in the North Atlantic region. These results have been obtained by means of different wavelet transforms (Cazelles et al., 2008; Grinsted et al., 2004; Labat, 2005), applied to a dense streamflow dataset spanning the years 1962 to 2012 (Vicente-Serrano et al., 2019).

Although the exploitation of wavelet transforms for hydrological analysis is not new, its application to spatially dense streamflow datasets is not common. In recent years, only a few studies (none of them in Europe) have addressed streamflow frequency analysis using wavelets on high spatial resolution databases. No consensus about a unique approach to summarize the results and the extraction of spatial patterns has arisen: streamflow frequency-based regionalization has been undertaken using k-means clustering Zoppou et al., 2002, principal component analysis (Saco and Kumar, 2000), multiscale entropy (Agarwal et al., 2016a) or self-organizing maps (Agarwal et al., 2016b). In the present study, the application of PCA to decomposed matrices representing the periodograms of each different wavelet power spectrum allowed us to unveil a regional change in streamflow frequencies with very coherent spatial patterns. The use of the SSI to standardize streamflow data prior to applying wavelet transforms (Huang et al., 2016; Li et al., 2019), enabled the inter comparison of results across a wide variety of basins and avoided the over estimation of significant power at the 1-year period, very common when streamflow data standardization is not accurate, or when data is not standardized at all (Grinsted et al., 2004; Su et al., 2019).

5.1. Observed changes in streamflow frequencies and climatic attribution

One of the main findings of this study is the generalized change in streamflow periodicities that occurred in most parts of the study area (following a gradient along the English Channel) between the mid of the 1980s and 2012. A change of streamflow frequency fluctuations from cycles shorter than 3 years, to the establishment of persistent fluctuations around cycles of 7 years since the 1980s, was identified. These findings confirm the results obtained by previous studies in individual river basins within the studied area, and broaden those insights using a high-resolution hydrological database. Massei et al. (2010) stressed the existence of fluctuations around the 5–9 years periods since the 1980s in discharge of the Seine river in northern France. (Labat, 2008) indicated dominant periods of 5–8 years in the Loire streamflow, and Franco-Villoria et al. (2012) also found streamflow cycles greater than 4 years in Scottish rivers, with a change point in streamflow dynamics in 1986, similar to the time of the most relevant changes identified in our study. Recently, Rust et al. (2020) found a general periodicity of 7 years in river discharges of Southeast England and Wales river basins.

Climate variability may have contributed to the observed changes in streamflow cycles. The large spatial extent of the changes suggest that it is not probable that local factors have determined the long term dynamics and periodicities. In addition, precipitation variability dominated by 7 year cycles was already observed in several locations of Ireland (Butler et al., 2007), England (Rust et al., 2019) and France (Hermida et al., 2015), reinforcing the idea that the hydrological change observed has a climatic origin.

5.2. Relationships between changes in streamflow periodicity and changes in the dominant atmospheric circulation mechanisms in the North Atlantic region

The changing conditions in the main atmospheric circulation mechanisms affecting the North Atlantic region have been documented in different studies. In particular, the changing dynamics of the NAO, as the main atmospheric mechanism in the North Atlantic region (Barnston and Livezey, 1987; Hurrell et al., 2003; Hurrell and Deser, 2009; Visbeck et al., 2001) may explain the periodicities in streamflow across western Europe. In the case of the NAO, the changing conditions are associated with a strengthening of the positive values of the index since 1980 (Kingston et al., 2006), and in changes in the position of the pressure centres that define the NAO (Vicente-Serrano and López-Moreno, 2008). Within the studied area, atmospheric dynamics influenced river discharges and groundwater levels, and these dynamics have already proven to exhibit non-stationary behaviour, driven by the coupling of different climate patterns, including the NAO, the EA and the SCAND patterns (Comas-Bru and McDermott, 2014; Holman et al., 2011; Machado et al., 2015; Neves et al., 2019; Rust et al., 2019). Nevertheless, several studies have also stressed a 7-year cycle in the fluctuations of the North Atlantic Oscillation during the last decades (Barbosa et al., 2006; Labat, 2010; Rust et al., 2019), which is consistent with our findings. We also show that the strengthening of the signal of the NAO index during the last three decades (Fig. 4a) likely explains the stronger correlations between monthly streamflows and winter NAO during the second half of the study period (1987–2012). In this context, the prominence of more positive phases of the NAO since the 1980s (Kingston et al., 2006; Visbeck et al., 2001) may explain the increased incidence of significant negative correlations with streamflow in the Iberian Peninsula and southeast France, the increase of positive correlations in northeast France and the southern England, and the disappearance of positive correlations in northern England and Scotland during the second half of the study period. This variability may be also the product of changes in the position of the NAO related pressure centres (Vicente-Serrano and López-Moreno, 2008).

These changing dynamics also in the NAO have coincided with changes in other atmospheric circulation mechanisms that control climate variability in the region, including a weakening in the EA signal in winter and autumn during the last decades (Iglesias et al., 2014). The links between the NAO and streamflow are not straightforward in many regions (e.g., Ireland, southern England, France; Comas-Bru and McDermott, 2014) which have undergone changes in the intensity and sign related to the transitive coupling between the main north Atlantic climate patterns. In this sense, the weakening of the EA since the 1980s have been accompanied by the temporary strengthening of the SCAND and EAWR patterns (Holman et al., 2011; Ionita, 2014). This coincidence with more powerful (as depicted by the wavelet analysis) phases of the SCAND and EAWR may have favoured the creation of the 7-years cycle in streamflow since the 1980s, especially in southern England and France. We show how significant correlations between streamflow and both climate patterns during wintertime have increased considerably in number during the second half of our study period. In this case, the increased intensity of the links between the SCAND and the EAWR patterns and streamflow may be related to changes in the position of the pressure centres associated with the re-configuration of pressure gradients, suggesting complex non-linear interactions between climate modes (Feldstein, 2000). On the contrary, significant correlations between the

SCAND and the EAWR summer indices decreased considerably in number during the second half of our study period (Figs. 7 and 8). This may explain why the contribution of the SCAND and EAWR patterns to explaining the generalized 7-years cycle was apparently restricted to the 1980s and 1990s, and the predominance of the NAO in the hydro-climatic coupling during the last two decades.

Our results also suggest that winter streamflow at low frequency periods in Ireland, Scotland, southern England and France are sensitive to different combinations between the NAO and coexisting SCAND and EAWR patterns. Since the middle of the 1980s, a transition towards the predominance of the NAO on streamflow and its frequencies is observed. The impacts on streamflow periodicities of this transitive coupling have already been related to the establishment of a 7-years cycle in the fluctuations of many aquifers in the UK (Rust et al., 2019). Neves et al. (2019) also observed strong co-variability between the NAO and groundwater levels of selected aquifers in Portugal around the 6–10 years period, and between groundwater levels and the SCAND pattern around 4–6 years. Our results are consistent with these findings and demonstrate that these time-frequency configurations of the hydrological variables and interactions with different climate patterns are not exclusive to groundwater levels, characterized by great inertia (Andreo et al., 2006; Lorenzo-Lacruz et al., 2017; Rust et al., 2019), but they also became the recent normal functioning of many river basins in the north Atlantic façade of Europe. The influence that these transitive couplings among indices (NAO, SCAND, EAWR) have had on streamflow generation during the last 30 years, is perhaps one of the most relevant results of our study, and highlights the great complexity associated with the non-stationary nature of many hydro-climatic interactions.

Among the limitations of the study, the most notable may be related to the short length of streamflow series (50 years), which introduces limitations when analysing frequencies and periodicities, and may not be the most appropriate for this task. In this sense, the objective was to obtain a dense (spatially) streamflow database, that allowed us to extract robust spatial patterns in the results obtained: in spite of the (a priori) short temporal span of the streamflow series, the spatial coherence is evident and the signal found in streamflow periodicities (7-years cycle) is coherent in most parts of the region and consistent with the results obtained in previous studies (Labat, 2008; Massei et al., 2010; Rust et al., 2020; Rust et al., 2021).

It is important to note that the very complex interactions between atmospheric circulation and streamflow exemplified here, may also be influenced by, at least, two types of lags: i) a natural lag occurring between the atmospheric/synoptic situation (and the associated meteorological conditions) and the generation of river discharges (runoff lag); and ii) an anthropogenic-induced lag, created by reservoirs in regulated basins (López-Moreno et al., 2013; Lorenzo-Lacruz et al., 2013a, 2013b, 2010). These lags may reduce the size of the bands and patches with significant coherence depicted by the WTC (correlation analogous) compared to those highlighted by the XWT analysis (covariance analogous). In any case, the XWT analysis shown in Fig. 9 has unveiled even more clear synchronicities around the 7-years cycle between western Europe streamflow and the dynamics of the NAO during the last two decades, and with those of the EAWR and SCAND patterns during the decades of the 1980s and 1990s.

It is also important to note that in the Iberian Peninsula, changes in streamflow frequencies are less intense and apparently, they are not related to atmospheric circulation mechanisms. The blurring of the 7-years streamflow cycle in the Iberian Peninsula may be caused by river regulation and water management. Spain is the European country with most dams regulating its rivers (approx. 1200), in a great portion, aimed to supply water to the enormous irrigated surface area (> 4,000,000 ha; Fig. 1). These alterations generate important changes in the periodicities and cycles of river discharges in the Iberian Peninsula. In highly regulated rivers, an annual periodicity is induced due to water demand during the irrigation period from May to October (Lorenzo-Lacruz et al., 2013b, 2012). Moreover, the reservoir system in Spain includes a wide range of water management strategies (as well as numerous water agencies), having multi-annual reservoirs responding to low frequency climatic variability (Lorenzo-Lacruz et al., 2010), or other types of reservoirs (or water management strategies) responding to higher frequency climatic variability (López-Moreno et al., 2013). The differences and inconsistencies in water management practices in a broad scale may introduce noise in the analysis, rather than a systematic signal or cycle detectable by the wavelet transforms, reinforcing the idea that the 7-years cycle detected is highly related to atmospheric dynamics and variability (Rust et al., 2021). The degree of complexity in understanding these processes is increased by the role of rising urban water demand, tourist water consumption and aquifer overexploitation (Brendel, 2020; Rupérez-Moreno et al., 2017; Tortajada et al., 2019). This complexity is compatible with the findings of the present study, with changes in Iberian streamflow frequencies showing a weaker association with changes in atmospheric circulation.

6. Conclusion and outlook

Effective future water resources management is threatened by the uncertainties related to changing climate processes and anthropogenic impacts that are occurring on an increasing basis, blurring the relationships in hydro-climatic interactions and feedbacks. For these reasons, water resources management must rely on the knowledge of the hydrological systems and the changing interactions with climate patterns and atmospheric circulation. In this study, we show for the first time at a continental scale, the existence of a generalized change in river discharge frequencies in western Europe, with the establishment of a cycle around the 7-years period in the fluctuations between high and low flow periods since the 1980s. We also show how the transitive coupling among the NAO, the SCAND and the EAWR patterns was responsible for the creation and sustainment of these periodicities, with a prominent role of the NAO during the last decades (Rust et al., 2021). These results confirm and broaden the insights obtained in previous studies, thanks to the high spatial resolution, robustness and quality of the data base used.

Wavelet transforms represent a promising tool for streamflow forecasting and the implementation of effective anticipatory water management strategies (Gürsoy and Engin, 2019; Hadi and Tombul, 2018; da Honorato et al., 2018). In this context, frequency statistics can be incorporated in to the development of drought early warning systems: the ability to pinpoint a discrete time period of sufficient stationarity (in this case, the 7-years cycle between the mid 1980s and 2012), may help to select a suitable calibration period for the improvement of the models (Yuan et al., 2017). All this may help to understand future hydrological behaviour and foresee the availability of water resources in many areas of the world, under a water scarcity scenario.

Authors contribution

SVS, JLL and JH designed the research; SVS, JH, CM, DPA and JLL elaborated the database; JLL, EMT and CG performed the formal analysis; JLL drafted the paper; JLL and EMT elaborated the figures; all the authors contributed to the writing and editing of the article.

Declaration of Competing Interest

The authors declare that they have no conflict of interest.

Acknowledgements

This work was supported by the research projects CGL2017-82216-R financed by the Spanish Commission of Science and Technology and FEDER, IMDROFLOOD financed by the WaterWorks 2014 co-funded call of the European Commission, CROSSDRO financed by the AXIS (Assessment of Cross(X) - sectorial climate Impacts and pathways for

Sustainable transformation) JPI-Climate co-funded call of the European Commission, INDECIS, which is part of ERA4CS, an ERA-NET initiated by JPI Climate, and funded by FORMAS (SE), DLR (DE), BMWFW (AT), IFD (DK), MINECO (ES), ANR (FR), FCT (PT) with co-funding by the European Union (Grant 690462). Author JLL was founded by Ministerio de Educación, Cultura y Deporte, Programa Estatal de Promoción del Talento y su Empleabilidad en I + D + I, Subprograma Estatal de Movilidad, del Plan Estatal de Investigación Científica y Técnica y de Innovación 2013-2016. JLL acknowledges the Centre for Ecology and Hydrology (NERC, Wallingford, UK) for hosting him during the spring of 2018. CM acknowledges funding from a Science Foundation Ireland Career Development Award SFI/17/CDA/4783.

References

Adamowski, J., Prokoph, A., 2014. Determining the amplitude and timing of streamflow discontinuities: a cross wavelet analysis approach. Hydrol. Process. 28, 2782–2793. https://doi.org/10.1002/hyp.9843.

Agarwal, A., Maheswaran, R., Kurths, J., Khosa, R., Manage, W.R., 2016a. Wavelet spectrum and self-organizing maps-based approach for hydrologic regionalization -a case study in the Western United States. Water Resour. Manag. https://doi.org/10.1007/s11269-016-1428-1.

Agarwal, A., Maheswaran, R., Sehgal, V., Khosa, R., Sivakumar, B., Bernhofer, C., 2016b. Hydrologic regionalization using wavelet-based multiscale entropy method. J. Hydrol. 538, 22–32. https://doi.org/10.1016/j.jhydrol.2016.03.023.

Agarwal, A., Marwan, N., Rathinasamy, M., Merz, B., Kurths, J., 2017. Multi-scale event synchronization analysis for unravelling climate processes: a wavelet-based approach. Nonlinear Proc. Geophys. Disc. 1–20 https://doi.org/10.5194/npg-2017-19.

Anctil, F., Coulibaly, P., 2004. Wavelet Analysis of the Interannual Variability in Southern Québec Streamflow. J. Clim. 17, 163–173. https://doi.org/10.1175/1520-0442(2004)017<0163:WAOTIV>2.0.CO;2.

Andreo, B., Jiménez, P., Durán, J.J., Carrasco, F., Vadillo, I., Mangin, A., 2006. Climatic and hydrological variations during the last 117-166 years in the south of the Iberian Peninsula, from spectral and correlation analyses and continuous wavelet analyses. J. Hydrol. 324, 24–39. https://doi.org/10.1016/j.jhydrol.2005.09.010.

Barbosa, S., Silva, M.E., Fernandes, M.J., 2006. Wavelet analysis of the Lisbon and Gibraltar North Atlantic Oscillation winter indices. Int. J. Climatol. 26, 581–593. https://doi.org/10.1002/joc.1263.

Barker, L.J., Hannaford, J., Chiverton, A., Svensson, C., 2016. From meteorological to hydrological drought using standardised indicators. Hydrol. Earth Syst. Sci. 20 (6), 2483–2505. https://doi.org/10.5194/hess-20-2483-2016.

Barnston, A.G., Livezey, R.E., 1987. Classification, seasonality and persistence of low-frequency atmospheric circulation patterns. Mon. Weather Rev. https://doi.org/10.1175/1520-0493(1987)115<1083:CSAPOL>2.0.CO;2.

Benner, T.C., 1999. Central England temperatures: lon-term variability and teleconnections. Int. J. Climatol. 19, 391–403.

Bierkens, M.F.P., Van Beek, L.P.H., 2009. Seasonal predictability of european discharge: NAO and hydrological response time. J. Hydrometeorol. 10, 953–968. https://doi.org/10.1175/2009JHM1034.1.

Blöschl, G., Hall, J., Viglione, A., Perdigão, R.A.P., Parajka, J., Merz, B., Lun, D., Arheimer, B., Aronica, G.T., Bilibashi, A., Boháč, M., Bonacci, O., Borga, M., Čanjevac, I., Castellarin, A., Chirico, G.B., Claps, P., Frolova, N., Ganora, D., Gorbachova, L., Gül, A., Hannaford, J., Harrigan, S., Kireeva, M., Kiss, A., Kjeldsen, T.R., Kohnová, S., Koskela, J.J., Ledvinka, O., Macdonald, N., Mavrova-Guirguinova, M., Mediero, L., Merz, R., Molnar, P., Montanari, A., Murphy, C., Osuch, M., Ovcharuk, V., Radevski, I., Salinas, J.L., Sauquet, E., Šraj, M., Szolgay, J., Volpi, E., Wilson, D., Zaimi, K., Živković, N., 2019. Changing climate both increases and decreases European river floods. Nature 573, 108–111. https://doi.org/10.1038/s41586-019-1495-6.

Brendel, B., 2020. Dam construction in Francoist Spain in the 1950s and 1960s: Negotiating the future and the past. Sustain. Dev. 28, 396–404. https://doi.org/10.1002/sd.1993.

Burt, T.P., Howden, N.J.K., 2013. North Atlantic Oscillation amplifies orographic precipitation and river flow in upland Britain. Water Resour. Res. 49, 3504–3515. https://doi.org/10.1002/wrcr.20297.

Butler, C.J., García-Suárez, A., Pallé, E., 2007. Trends and cycles in long Irish meteorological series. Biol. Environ. 107, 157–165. https://doi.org/10.3318/BIOE.2007.107.3.157.

Cazelles, B., Chavez, M., Berteaux, D., Ménard, F., Vik, J.O., Jenouvrier, S., Stenseth, N. C., 2008. Wavelet analysis of ecological time series. Oecologia 156, 287–304. https://doi.org/10.1007/s00442-008-0993-2.

Comas-Bru, L., McDermott, F., 2014. Impacts of the EA and SCA patterns on the European twentieth century NAO-winter climate relationship. Q. J. R. Meteorol. Soc. 140, 354–363. https://doi.org/10.1002/qj.2158.

da Honorato, A.G.S.M., da Silva, G.B.L., Guimarães Santos, C.A., 2018. Monthly streamflow forecasting using neuro-wavelet techniques and input analysis. Hydrol. Sci. J. 63, 2060–2075. https://doi.org/10.1080/02626667.2018.1552788.

De Vita, P., Allocca, V., Manna, F., Fabbrocino, S., 2012. Coupled decadal variability of the North Atlantic Oscillation, regional rainfall and karst spring discharges in the Campania region (southern Italy). Hydrol. Earth Syst. Sci. 16, 1389–1399. https://doi.org/10.5194/hess-16-1389-2012.

Farge, M., 1992. Wavelet transforms and their applications to turbulence. Annu. Rev. Fluid Mech. 24, 395–457.

Feldstein, S.B., 2000. The Timescale, Power Spectra, and climate Noise Properties of Teleconnection patterns. J. Clim. 13, 4430–4440. https://doi.org/10.1175/1520-0442(2000)013<4430:TTPSAC>2.0.CO;2.

Franco-Villoria, M., Scott, M., Hoey, T., Fischbacher-Smith, D., 2012. Temporal investigation of flow variability in Scottish Rivers using wavelet analysis. J. Environ. Stat. 3 (6), 1–20.

García-Herrera, R., Hernández, E., Barriopedro, D., Paredes, D., Trigo, R.M., Trigo, I.F., Mendes, M.A., 2007. The outstanding 2004/05 Drought in the Iberian Peninsula: Associated Atmospheric Circulation. J. Hydrometeorol. 8, 483–498. https://doi.org/10.1175/JHM578.1.

García-Ruiz, J.M., López-Moreno, I.I., Vicente-Serrano, S.M., Lasanta-Martínez, T., Beguería, S., 2011. Mediterranean water resources in a global change scenario. Earth Sci. Rev. 105, 121–139. https://doi.org/10.1016/j.earscirev.2011.01.006.

Gouhier, T.C., Grinsted, A., Simko, V., Tarik, M., Gouhier, C., 2016. biwavelet R package.

Grinsted, A., Moore, J.C., Jevrejeva, S., 2004. Application of the cross wavelet transform and wavelet coherence to geophysical time series. Nonlinear Processes in Geophysics, European Geosciences Union 11, 561–566.

Gudmundsson, L., Seneviratne, S.I., Xuebin, Z., 2017. Anthropogenic climate change detected in European renewable freshwater resources. Nat. Clim. Chang. 7, 813–816.

Gürsoy, Ö., Engin, S.N., 2019. A wavelet neural network approach to predict daily river discharge using meteorological data. Measure. Control 52, 599–607. https://doi.org/10.1177/0020294019827972.

Hadi, S.J., Tombul, M., 2018. Streamflow forecasting using four wavelet transformation combinations approaches with data-driven models: a comparative study. Water Resour. Manag. 32, 4661–4679. https://doi.org/10.1007/s11269-018-2077-3.

Hannaford, J., 2015. Climate-driven changes in UK river flows: a review of the evidence. Prog. Phys. Geogr. 39, 29–48. https://doi.org/10.1177/0309133314536755.

Hannaford, J., Buys, G., 2012. Trends in seasonal river flow regimes in the UK. J. Hydrol. 475, 158–174. https://doi.org/10.1016/j.jhydrol.2012.09.044.

Hannaford, J., Marsh, T., 2006. An assessment of trends in UK runoff and low flows using a network of undisturbed catchments. Int. J. Climatol. 26, 1237–1253. https://doi.org/10.1002/joc.1303.

Hannaford, J., Lloyd-Hughes, B., Keef, C., Parry, S., Prudhomme, C., 2011. Examining the large-scale spatial coherence of European drought using regional indicators of precipitation and streamflow deficit. Hydrol. Process. 25, 1146–1162. https://doi.org/10.1002/hyp.7725.

Harrigan, S., Murphy, C., Hall, J., Wilby, R.L., Sweeney, J., 2014. Attribution of detected changes in streamflow using multiple working hypotheses. Hydrol. Earth Syst. Sci. 18, 1935–1952. https://doi.org/10.5194/hess-18-1935-2014.

Haunschild, R., Bornmann, L., Marx, W., 2016. Climate change research in view of bibliometrics. PLoS One 11, e0160393. https://doi.org/10.1371/journal.pone.0160393.

Hermida, L., López, L., Merino, A., Berthet, C., García-Ortega, E., Sánchez, J.L., Dessens, J., 2015. Hailfall in Southwest France: Relationship with precipitation, trends and wavelet analysis. Atmos. Res. 156, 174–188. https://doi.org/10.1016/j.atmosres.2015.01.005.

Hernández, A., Trigo, R.M., Pla-Rabes, S., Valero-Garcés, B.L., Jerez, S., Rico-Herrero, M., Vega, J.C., Jambrina-Enríquez, M., Giralt, S., 2015. Sensitivity of two Iberian lakes to North Atlantic atmospheric circulation modes. Clim. Dyn. 45, 3403–3417. https://doi.org/10.1007/s00382-015-2547-8.

Hisdal, H., Stahl, K., Tallaksen, L.M., Demuth, S., 2001. Have streamflow droughts in Europe become more severe or frequent? Int. J. Climatol. 21, 317–333. https://doi.org/10.1002/joc.619.

Holman, I.P., Rivas-Casado, M., Bloomfield, J.P., Gurdak, J.J., 2011. Identifying non-stationary groundwater level response to North Atlantic Ocean-atmosphere teleconnection patterns using wavelet coherence. Hydrogeol. J. 19, 1269–1278. https://doi.org/10.1007/s10040-011-0755-9.

Huang, S., Huang, Q., Chang, J., Leng, G., 2016. Linkages between hydrological drought, climate indices and human activities: a case study in the Columbia River basin. Int. J. Climatol. 36, 280–290. https://doi.org/10.1002/joc.4344.

Hurrell, J.W., Deser, C., 2009. North Atlantic climate variability: the role of the North Atlantic Oscillation. J. Mar. Syst. 78, 28–41. https://doi.org/10.1016/j.jmarsys.2008.11.026.

Hurrell, J.W., Van Loon, H., 1997. Decadal variations in climate associated with the North Atlantic Oscillation. Clim. Chang. 36, 301–326. https://doi.org/10.1023/a:1005314315270.

Hurrell, J.W., Kushnir, Y., Otterson, G., Visbeck, M., 2003. An Overview of the North Atlantic Oscillation. In: The North Atlantic Oscillation: Climatic Significance and Environmental Impact, 134, p. 263. https://doi.org/10.1029/GM134.

Iglesias, I., Lorenzo, M.N., Taboada, J.J., 2014. Seasonal predictability of the East Atlantic pattern from sea surface temperatures. PLoS One 9, 1–8. https://doi.org/10.1371/journal.pone.0086439.

Ionita, M., 2014. The impact of the East Atlantic/Western Russia pattern on the hydroclimatology of Europe from mid-winter to late spring. Climate 2, 296–309. https://doi.org/10.3390/cli2040296.

Kahya, E., Kalayci, S., 2004. Trend analysis of streamflow in Turkey. J. Hydrol. 289, 128–144. https://doi.org/10.1016/j.jhydrol.2003.11.006.

Kalimeris, A., Ranieri, E., Founda, D., Norrant, C., 2017. Variability modes of precipitation along a Central Mediterranean area and their relations with ENSO, NAO, and other climatic patterns. Atmos. Res. 198, 56–80. https://doi.org/10.1016/J.ATMOSRES.2017.07.031.

Kiely, G., 1999. Climate change in Ireland from precipitation and streamflow observations. Adv. Water Resour. 23, 141–151. https://doi.org/10.1016/S0309-1708(99)00018-4.

Kingston, D.G., Lawler, D.M., McGregor, G.R., 2006. Linkages between atmospheric circulation, climate and streamflow in the northern North Atlantic: research prospects. Prog. Phys. Geogr. 30, 143–174. https://doi.org/10.1191/0309133306pp471ra.

Krichak, S.O., Alpert, P., 2005. Decadal trends in the east Atlantic–west Russia pattern and Mediterranean precipitation. Int. J. Climatol. 25, 183–192. https://doi.org/10.1002/joc.1124.

Labat, D., 2005. Recent advances in wavelet analyses: part 1. A review of concepts. J. Hydrol. 314, 275–288.

Labat, D., 2006. Oscillations in land surface hydrological cycle. Earth Planet. Sci. Lett. 242, 143–154.

Labat, D., 2008. Wavelet analysis of the annual discharge records of the world's largest rivers. Adv. Water Resour. 31, 109–117. https://doi.org/10.1016/j.advwatres.2007.07.004.

Labat, D., 2010. Cross wavelet analyses of annual continental freshwater discharge and selected climate indices. J. Hydrol. 385, 269–278.

Li, Q., He, P., He, Y., Han, X., Zeng, T., Lu, G., Wang, H., 2019. Investigation to the relation between meteorological drought and hydrological drought in the upper Shaying River Basin using wavelet analysis. Atmos. Res. 104743 https://doi.org/10.1016/j.atmosres.2019.104743.

Liu, Y., San Liang, X., Weisberg, R.H., Liu, Y., Liang, X.S., Weisberg, R.H., 2007. Rectification of the Bias in the Wavelet Power Spectrum. J. Atmos. Ocean. Technol. 24, 2093–2102. https://doi.org/10.1175/2007JTECHO511.1.

López-Moreno, J.I., Vicente-Serrano, S.M., Zabalza, J., Beguería, S., Lorenzo-Lacruz, J., Azorin-Molina, C., Moran-Tejeda, E., 2013. Hydrological response to climate variability at different time scales: a study in the Ebro basin. J. Hydrol. 477, 175–188. https://doi.org/10.1016/j.jhydrol.2012.11.028.

Lorenzo-Lacruz, J., Vicente-Serrano, S.M., López-Moreno, J.I., Beguería, S., García-Ruiz, J.M., Cuadrat, J.M., 2010. The impact of droughts and water management on various hydrological systems in the headwaters of the Tagus River (Central Spain). J. Hydrol. 386, 13–26. https://doi.org/10.1016/j.jhydrol.2010.01.001.

Lorenzo-Lacruz, J., Vicente-Serrano, S.M., López-Moreno, J.I., González-Hidalgo, J.C., Morán-Tejeda, E., 2011. The response of Iberian rivers to the North Atlantic Oscillation. Hydrol. Earth Syst. Sci. 15 https://doi.org/10.5194/hess-15-2581-2011.

Lorenzo-Lacruz, J., Vicente-Serrano, S.M., López-Moreno, J.I., Morán-Tejeda, E., Zabalza, J., 2012. Recent trends in Iberian streamflows (1945-2005). J. Hydrol. 414–415, 463–475. https://doi.org/10.1016/j.jhydrol.2011.11.023.

Lorenzo-Lacruz, J., Moran-Tejeda, E., Vicente-Serrano, S.M., López-Moreno, J.I., 2013a. Streamflow droughts in the Iberian Peninsula between 1945 and 2005: spatial and temporal patterns. Hydrol. Earth Syst. Sci. 17, 119–134. https://doi.org/10.5194/hess-17-119-2013.

Lorenzo-Lacruz, J., Vicente-Serrano, S.M., González-Hidalgo, J.C., López-Moreno, J.I., Cortesi, N., 2013b. Hydrological drought response to meteorological drought in the Iberian Peninsula. Clim. Res. 58, 117–131. https://doi.org/10.3354/cr01177.

Lorenzo-Lacruz, J., Garcia, C., Morán-Tejeda, E., 2017. Groundwater level responses to precipitation variability in Mediterranean insular aquifers. J. Hydrol. https://doi.org/10.1016/j.jhydrol.2017.07.011.

Luque-Espinar, J.A., Chica-Olmo, M., Pardo-Igúzquiza, E., García-Soldado, M.J., 2008. Influence of climatological cycles on hydraulic heads across a Spanish aquifer. J. Hydrol. 354, 33–52. https://doi.org/10.1016/J.JHYDROL.2008.02.014.

Machado, M.J., Botero, B.A., López, J., Francés, F., Díez-Herrero, A., Benito, G., 2015. Flood frequency analysis of historical flood data under stationary and non-stationary modelling. Hydrol. Earth Syst. Sci. 19, 2561–2576. https://doi.org/10.5194/hess-19-2561-2015.

Maheswaran, R., Khosa, R., 2012. Comparative study of different wavelets for hydrologic forecasting. Comput. Geosci. 46, 284–295. https://doi.org/10.1016/J.CAGEO.2011.12.015.

Massei, N., Durand, A., Deloffre, J., Dupont, J.P., Valdes, D., Laignel, B., Massei, C., 2007. Investigating possible links between the North Atlantic Oscillation and rainfall variability in northwestern France over the past 35 years. J. Geophys. Res. 112, 9121. https://doi.org/10.1029/2005JD007000.

Massei, N., Laignel, B., Deloffre, J., Mesquita, J., Motelay, A., Lafite, R., Durand, A., 2010. Long-term hydrological changes of the Seine River flow (France) and their relation to the North Atlantic Oscillation over the period 1950-2008. Int. J. Climatol. 30, 2146–2154. https://doi.org/10.1002/joc.2022.

Masseroni, D., Camici, S., Cislaghi, A., Vacchiano, G., Massari, C., Brocca, L., 2020. 65-year changes of annual streamflow volumes across Europe with a focus on the Mediterranean basin. Hydrol. Earth Syst. Sci. Discuss. 1–16 https://doi.org/10.5194/hess-2020-21.

Milly, A.P.C.D., Betancourt, J., Falkenmark, M., Hirsch, R.M., Zbigniew, W., Lettenmaier, D.P., Stouffer, R.J., Milly, P.C.D., 2008. Stationarity is dead: stationarity whither water management ? Science 319, 573–574. https://doi.org/10.1126/science.1151915.

Moore, G.W.K., Renfrew, I.A., Pickart, R.S., 2013. Multidecadal mobility of the North Atlantic Oscillation. J. Clim. 26, 2453–2466. https://doi.org/10.1175/JCLI-D-12-00023.1.

Morán-Tejeda, E., Ignacio, L.M., Antonio, C.B., Sergio, M.V.S., 2011. Evaluating Duero's basin (Spain) response to the NAO phases: Spatial and seasonal variability. Hydrol. Process. 25, 1313–1326. https://doi.org/10.1002/hyp.7907.

Morán-Tejeda, E., Ceballos-Barbancho, A., Llorente-Pinto, J.M., López-Moreno, J.I., 2012. Land-cover changes and recent hydrological evolution in the Duero Basin (Spain). Reg. Environ. Chang. 12, 17–33. https://doi.org/10.1007/s10113-011-0236-7.

Neves, M.C., Jerez, S., Trigo, R.M., 2019. The response of piezometric levels in Portugal to NAO, EA, and SCAND climate patterns. J. Hydrol. 568, 1105–1117. https://doi.org/10.1016/j.jhydrol.2018.11.054.

Özger, M., Mishra, A.K., Singh, V.P., 2009. Low frequency drought variability associated with climate indices. J. Hydrol. 364, 152–162. https://doi.org/10.1016/j.jhydrol.2008.10.018.

Pekárová, P., Pekar, J., 2004. Teleconnections of AO, NAO, SO, and QBO with interannual streamflow fluctuation in the Hron Basin. J. Hydrol. Hydromech. 52, 279–290.

Peña-Gallardo, M., Vicente-Serrano, S.M., Hannaford, J., Lorenzo-Lacruz, J., Svoboda, M., Domínguez-Castro, F., Maneta, M., Tomas-Burguera, M., El Kenawy, A., 2019. Complex influences of meteorological drought time-scales on hydrological droughts in natural basins of the contiguous Unites States. J. Hydrol. 568, 611–625. https://doi.org/10.1016/j.jhydrol.2018.11.026.

Revelle, W., 2021. Package "Psych": Procedures for Psychological, Psychometric, and Personality Research.

Richman, M.B., 1986. Rotation of principal components. J. Climatol. 6, 293–335. https://doi.org/10.1002/joc.3370060305.

Rösch, A., Schmidbauer, H., 2014. WaveletComp: A Guided Tour through the R-Package.

Rupérez-Moreno, C., Senent-Aparicio, J., Martinez-Vicente, D., García-Aróstegui, J.L., Calvo-Rubio, F.C., Pérez-Sánchez, J., 2017. Sustainability of irrigated agriculture with overexploited aquifers: the case of Segura basin (SE, Spain). Agric. Water Manag. 182, 67–76. https://doi.org/10.1016/j.agwat.2016.12.008.

Rust, W., Holman, I., Bloomfield, J., Cuthbert, M., Corstanje, R., 2019. Understanding the potential of climate teleconnections to project future groundwater drought. Hydrol. Earth Syst. Sci. 23, 3233–3245. https://doi.org/10.5194/hess-23-3233-2019.

Rust, W., Bloomfield, J., Cuthbert, M., Corstanje, R., Holman, I., 2021. The importance of non-stationary multiannual periodicities in the NAO index for forecasting water resource extremes. Hydrol. Earth Syst. Sci. Discuss. https://doi.org/10.5194/hess-2021-572 in review.

Rust, W., Cuthbert, M., Bloomfield, J., Corstanje, R., Howden, N., Holman, I., 2020. Exploring the role of hydrological pathways in modulating North Atlantic Oscillation (NAO) teleconnection periodicities from UK rainfall to streamflow. Hydrol. Earth Syst. Sci. Discuss. 1–26. https://doi.org/10.5194/hess-2020-312.

Saco, P., Kumar, P., 2000. Coherent modes in multiscale variability of streamflow over the United States. Water Resour. Res. 36 (4), 1049–1067. https://doi.org/10.1029/1999WR900345.

Sadri, S., Kam, J., Sheffield, J., 2016. Nonstationarity of low flows and their timing in the eastern United States. Hydrol. Earth Syst. Sci. 20, 633–649. https://doi.org/10.5194/hess-20-633-2016.

Slimani, S., Massei, N., Mesquita, J., Valdés, D., Fournier, M., Laignel, B., Dupont, J.-P., 2009. Combined climatic and geological forcings on the spatio-temporal variability of piezometric levels in the chalk aquifer of Upper Normandy (France) at pluridecennal scale. Hydrogeol. J. 17, 1823–1832. https://doi.org/10.1007/s10040-009-0488-1.

Stahl, K., Hisdal, H., Hannaford, J., Tallaksen, L.M., Van Lanen, H.A.J., Sauquet, E., Demuth, S., Fendekova, M., Jodar, J., 2010. Streamflow trends in Europe: evidence from a dataset of near-natural catchments. Hydrol. Earth Syst. Sci. 14, 2367–2382. https://doi.org/10.5194/hess-14-2367-2010.

Steirou, E., Gerlitz, L., Apel, H., Merz, B., 2017. Links between large-scale circulation patterns and streamflow in Central Europe: a review. J. Hydrol. 549, 484–500. https://doi.org/10.1016/j.jhydrol.2017.04.003.

Su, L., Miao, C., Duan, Q., Lei, X., Li, H., 2019. Multiple-wavelet coherence of world's large rivers with meteorological factors and ocean signals. J. Geophys. Res.-Atmos., 2018JD029842 https://doi.org/10.1029/2018JD029842.

Tamaddun, K.A., Kalra, A., Ahmad, S., 2017. Wavelet analyses of western US streamflow with ENSO and PDO. J. Water Clim. Change 8, 26–39. https://doi.org/10.2166/wcc.2016.162.

Telesca, L., Lovallo, M., Lopez-Moreno, I., Vicente-Serrano, S., 2012. Investigation of scaling properties in monthly streamflow and Standardized Streamflow Index (SSI) time series in the Ebro basin (Spain). Phys. A. 391, 1662–1678. https://doi.org/10.1016/j.physa.2011.10.023.

Teuling, A.J., De Badts, E., Jansen, F.A., Fuchs, R., Buitink, J., Hoek, A.J., Dijke, V., Sterling, S., 2019. Climate Change, Re- / Afforestation, and Urbanisation Impacts on Evapotranspiration and Streamflow in Europe 1–30.

Torrence, C., Compo, Gilbert, 1998. A Practical Guide to Wavelet Analysis. Bull. Am. Meteorol. Soc. 79, 61–78. https://doi.org/10.1175/1520-0477(1998)079<0061:APGTWA>2.0.CO;2.

Torrence, C., Webster, P.J., 1999. Interdecadal changes in the ENSO–Monsoon System. J. Clim. 12, 2679–2690.

Tortajada, C., González-gómez, F., Biswas, A.K., Buurman, J., 2019. Water demand management strategies for water-scarce cities: the case of Spain. Sustain. Cities Soc. 45, 649–656. https://doi.org/10.1016/j.scs.2018.11.044.

Trigo, R.M., Osborn, T.J., Corte-real, J.M., 2002. The North Atlantic Oscillation influence on Europe: climate impacts and associated physical mechanisms. Clim. Res. 20, 9–17. https://doi.org/10.3354/cr020009.

Trigo, R.M., Pozo-Vázquez, D., Osborn, T.J., Castro-Díez, Y., Gámiz-Fortis, S., Esteban-Parra, M.J., 2004. North Atlantic oscillation influence on precipitation, river flow and water resources in the Iberian Peninsula. Int. J. Climatol. 24, 925–944. https://doi.org/10.1002/joc.1048.

Van Loon, A.F., Van Huijgevoort, M.H.J., Van Lanen, H.A.J., 2012. Evaluation of drought propagation in an ensemble mean of large-scale hydrological models. Hydrol. Earth Syst. Sci. 16, 4057–4078. https://doi.org/10.5194/hess-16-4057-2012.

Veleda, D., Montagne, R., Araujo, M., Veleda, D., Montagne, R., Araujo, M., 2012. Cross-wavelet bias corrected by normalizing scales. J. Atmos. Ocean. Technol. 29, 1401–1408. https://doi.org/10.1175/JTECH-D-11-00140.1.

Vicente-Serrano, S.M., López-Moreno, J.I., 2008. Nonstationary influence of the North Atlantic Oscillation on European precipitation. J. Geophys. Res.-Atmos. 113, 1–14. https://doi.org/10.1029/2008JD010382.

Vicente-Serrano, Sergio M., López-Moreno, J.I., Drumond, A., Gimeno, L., Nieto, R., Morán-Tejeda, E., Lorenzo-Lacruz, J., Beguería, S., Zabalza, J., 2011a. Effects of warming processes on droughts and water resources in the NW Iberian Peninsula (1930-2006). Clim. Res. 48, 203–212. https://doi.org/10.3354/cr01002.

Vicente-Serrano, S.M., Trigo, R.M., López-Moreno, J.I., Liberato, M.L.R., Lorenzo-Lacruz, J., Beguería, S., Moran-Tejeda, E., El Kenawy, A., 2011b. Extreme winter precipitation in the Iberian Peninsula in 2010: anomalies, driving mechanisms and future projections. Clim. Res. 46, 51–65. https://doi.org/10.3354/cr00977.

Vicente-Serrano, S.M., López-Moreno, J.I., Beguería, S., Lorenzo-Lacruz, J., Azorin-Molina, C., Morán-Tejeda, E., 2012. Accurate computation of a streamflow drought index. J. Hydrol. Eng. 17, 318–332. https://doi.org/10.1061/(ASCE)HE.1943-5584.0000433.

Vicente-Serrano, S.M., Lopez-Moreno, J.-I., Beguería, S., Lorenzo-Lacruz, J., Sanchez-Lorenzo, A., García-Ruiz, J.M., Azorin-Molina, C., Moran-Tejeda, E., Revuelto, J., Trigo, R.M., Coelho, F., Espejo, F., 2014. Evidence of increasing drought severity caused by temperature rise in southern Europe. Environ. Res. Lett. 9, 044001 https://doi.org/10.1088/1748-9326/9/4/044001.

Vicente-Serrano, S.M., García-Herrera, R., Barriopedro, D., Azorin-Molina, C., López-Moreno, J.I., Martín-Hernández, N., Tomás-Burguera, M., Gimeno, L., Nieto, R., 2016. The Westerly Index as complementary indicator of the North Atlantic oscillation in explaining drought variability across Europe. Clim. Dyn. 47, 845–863. https://doi.org/10.1007/s00382-015-2875-8.

Vicente-Serrano, S.M., Zabalza-Martínez, J., Borràs, G., López-Moreno, J.I., Pla, E., Pascual, D., Savé, R., Biel, C., Funes, I., Azorin-Molina, C., Sanchez-Lorenzo, A., Martín-Hernández, N., Peña-Gallardo, M., Alonso-González, E., Tomas-Burguera, M., El Kenawy, A., 2017. Extreme hydrological events and the influence of reservoirs in a highly regulated river basin of northeastern Spain. J. Hydrol. Reg. Stud. 12, 13–32. https://doi.org/10.1016/J.EJRH.2017.01.004.

Vicente-Serrano, S.M., Peña-Gallardo, M., Hannaford, J., Murphy, C., Lorenzo-Lacruz, J., Dominguez-Castro, F., López-Moreno, J.I., Beguería, S., Noguera, I., Harrigan, S., Vidal, J.-P., 2019. Climate, irrigation, and land-cover change explain streamflow trends in countries bordering the Northeast Atlantic. Geophys. Res. Lett. 2019GL084084 https://doi.org/10.1029/2019GL084084.

Visbeck, M.H., Hurrell, J.W., Polvani, L., Cullen, H.M., 2001. The North Atlantic Oscillation: past, present, and future. Proc. Natl. Acad. Sci. U. S. A. 98, 12876–12877. https://doi.org/10.1073/pnas.231391598.

Wan, W., Zhao, J., Li, H.-Y., Mishra, A., Ruby Leung, L., Hejazi, M., Wang, W., Lu, H., Deng, Z., Demissisie, Y., Wang, H., 2017. Hydrological drought in the Anthropocene: impacts of local water extraction and reservoir regulation in the US. J. Geophys. Res.-Atmos. https://doi.org/10.1002/2017JD026899.

Wilby, R.L., 2001. Seasonal forecasting of River Flows in the British Isles using North Atlantic pressure patterns. Water Environ. J. 15, 56–63. https://doi.org/10.1111/j.1747-6593.2001.tb00305.x.

Wrzesiński, D., Paluszkiewicz, R., 2011. Spatial differences in the impact of the North Atlantic Oscillation on the flow of rivers in Europe. Hydrol. Res. 42, 30–39. https://doi.org/10.2166/nh.2010.077.

Yuan, X., Zhang, M., Wang, L., Zhou, T., 2017. Understanding and seasonal forecasting of hydrological drought in the Anthropocene. Hydrol. Earth Syst. Sci. 21, 5477–5492. https://doi.org/10.5194/hess-21-5477-2017.

Zaidman, M.D., Rees, H.G., Young, A.R., 2002. Spatio-temporal development of streamflow droughts in north-West Europe. Hydrol. Earth Syst. Sci. 6, 733–751.

Zhang, Q., Xu, C. Yu, Jiang, T., Wu, Y., 2007. Possible influence of ENSO on annual maximum streamflow of the Yangtze River, China. J. Hydrol. 333, 265–274. https://doi.org/10.1016/j.jhydrol.2006.08.010.

Zoppou, C., Nielsen, O.M., Zhang, L., 2002. Regionalization of daily streamflow in Australia using wavelets and k-means analysis; CMA Research Report MRR02-003. Australian National University, Canberra, Australia.